TEXACO

EXPERIMENT INCORPORATED

RICHMOND 2, VIRGINIA

EXP 328

14 April 1963

KINETICS OF CONDENSATION FROM THE VAPOR PHASE

Final Report

TM - 1377

Welby G. Courtney

TEXACO EXPERIMENT INCORPORATED
Richmond 2, Virginia

Submitted to the
Department of the Navy, Office of Naval Research
under Contract NOnr-3141(00)

CONTENTS

FIGURES

FIGURES (cont'd)

SUMMARY

This program is a theoretical and experimental investigation of the kinetics and mechanisms of condensation and particularly of homogeneous nucleation from the vapor phase.

Theoretical results are reported for (a) the rate of formation of solid H_2O drops during condensation under constant-volume conditions, (b) the rate of steady-state nucleation from a hypothetical complex vapor system using Li-F data as a base point and arbitrary rate constants, (c) the rate of condensation in generalized B_2O_3 and LiF systems, and (d) the corresponding rates of condensation in certain B-O-H and Li-F systems in a rocket nozzle.

Semiquantitative comparison of the experimental light-scattering-time curves obtained in the present cloud chamber with the previously reported theoretical curves continues to suggest that the present experimental results can be adequately interpreted by the classical liquid-drop theory of homogeneous nucleation together with collision-frequency growth kinetics. This comparison includes the effect of supersaturation and temperature. The experimental rates of condensation are slightly faster with lower concentration of inert gas (the previously reported opposite conclusion was incorrect). This trend qualitatively agrees with the above theory. The author, now located elsewhere, expects to make theoretical computations to test this effect of pressure semiquantitatively and these are expected to be reported later. The mathematical theory required to permit quantitative comparison between experimental and theoretical rates of condensation is given, but the comparison was not made. In view of the incomplete analysis, the raw data from the experimental pressure-time curves obtained during condensation in the cloud chamber used in this work are included in the Appendix.

This is the final report in a series of reports generated under contract NOnr-3141(00).

INTRODUCTION

The present program is a fundamental investigation of the kinetics and mechanisms of condensation and particularly of homogeneous nucleation from the vapor phase. A brief review of the program and accomplishments was given in reference 1.

This report is the final in a series of reports generated under contract NOnr-3141(00) and covers the period from about June 1 to August 17, 1962. Previous reports are listed as references 1 and 2.

The first section of this present report gives the completed current theoretical results and includes (a) computer analysis of the rate of steady-state nucleation in a complex Li-F vapor system, (b) computer analysis of the rate of condensation of B_2O_3 and LiF liquids, and (c) application of these latter condensation rates to rocket nozzles. The second section presents current but incomplete results of the experimental cloud-chamber work which investigated the rate of condensation of water vapor. In view of the incomplete analysis of the experimental results, raw experimental data are given in the Appendix.

No further work is anticipated on this contract because of the departure of the principal investigator from Texaco Experiment Incorporated. However, the author plans to carry out brief computer calculations of the effect of inert gas on rate of condensation of water and to continue analysis of the experimental data at his new location.* The data presented here are believed to be correct, but the interpretation of the results is provisional.

---

* Present address: Reaction Motors Division, Thiokol Chemical Corporation, Denville, New Jersey.

THEORY

Rate of Formation of Solid H_2O Particles

Figures 1 to 3 show the rate of formation of solid H_2O particles by the liquid-drop theory at -40, -60, and -80°C. These results were taken from the previously reported computer results (1).

Lack of time did not permit incorporating the lower limit to the classical liquid-drop theory, and these figures may use supersaturations for which the theoretical g^*, the number of molecules in the liquid-drop nucleus, is less than 20.

Steady-state Nucleation from Complex Systems

The previous summary report (pp. 48-61 of reference 1) examined the problem of the kinetics of nucleation from a complex vapor system and derived theoretical equations for complex nucleation kinetics (Equations 99-102 of reference 1).

Computer solution of these equations was done to check the theoretical formulation of the equations and also hopefully to gain some insight into the relative importance of the magnitude of the various input data. Since no information is available about any of the chemical reaction rates, extensive computer work did not seem warranted.

Specifically, the kinetics of nucleation of LiF(l) from a $LiF\text{-}(LiF)_2\text{-}(LiF)_3\text{-}LiX$ vapor system was examined at 1000°K by solving the referenced equations on a General Precision RPC 4000 Computer at TEI. Here, X is an "inert" atom such that

$$LiX + F = LiF(v) + X$$

Input data for σ and ρ for LiF(l) and the JANAF data for the equilibrium vapor concentrations of monomer, dimer, and trimer were reported previously.

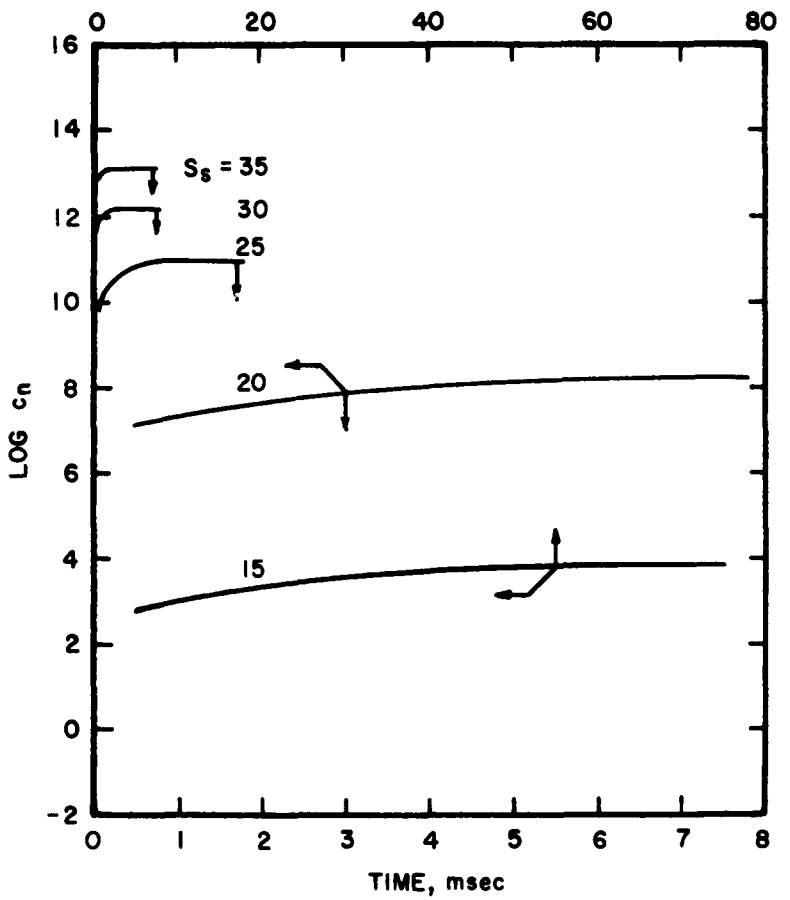

FIGURE I. RATE OF FORMATION OF SOLID H_2O PARTICLES BY LIQUID-DROP THEORY AT -40°C

S_s IS SUPERSATURATION WITH RESPECT TO BULK SOLID

c_n IS IN PARTICLES/CM^3

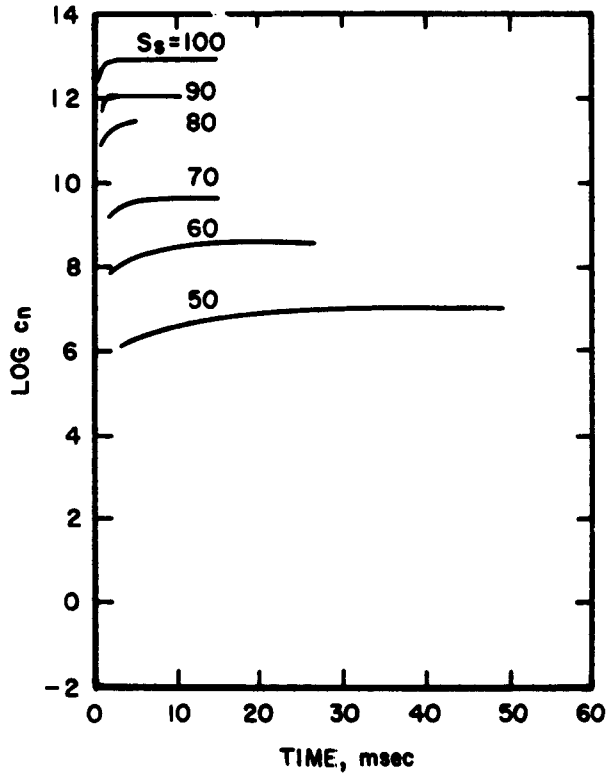

FIGURE 2. RATE OF FORMATION OF SOLID H_2O PARTICLES BY LIQUID-DROP THEORY AT -60°C

S_s IS SUPERSATURATION WITH RESPECT TO BULK SOLID

c_n IS IN PARTICLES/CM^3

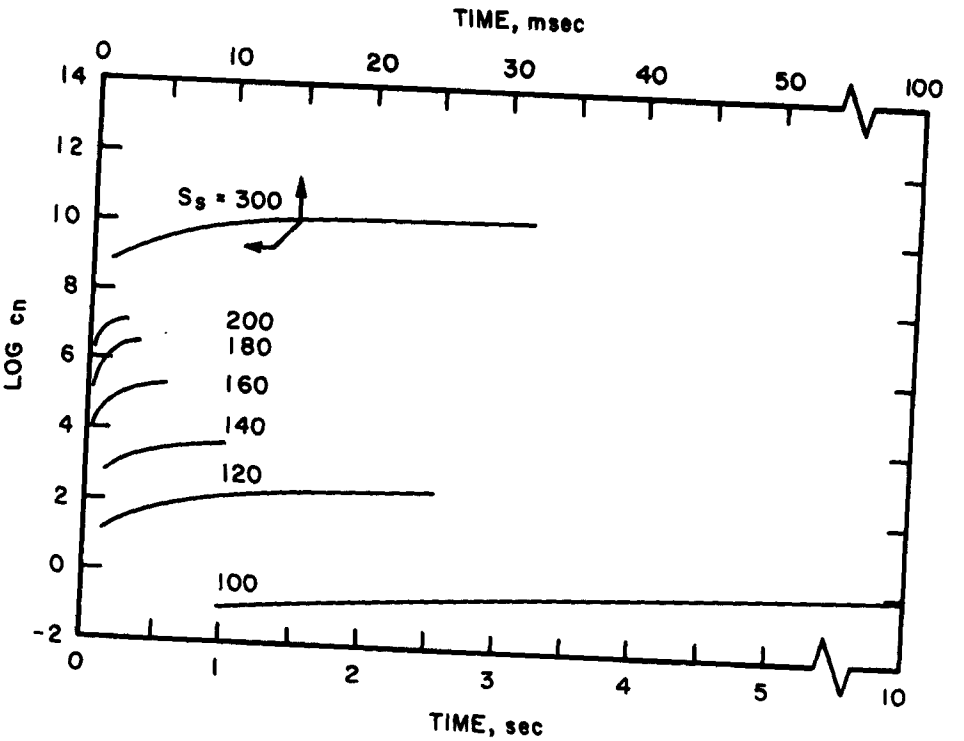

FIGURE 3. RATE OF FORMATION OF SOLID H_2O PARTICLES BY LIQUID-DROP THEORY AT -80°C

S_s IS SUPERSATURATION WITH RESPECT TO BULK SOLID

c_n IS IN PARTICLES / CM^3

The general mathematical approach was to compute $(R_s)_g$ (the approximate value of the steady-state homogeneous nucleation rate for the nonequilibrated vapor) for the complex system for successive values of g, where g is the number of LiF molecules in the cluster under consideration. The variation in $(R_s)_g$ with increasing g was noted, and the steady-state rate of nucleation for the complex system, $(R_s)_{complex}$, was taken as the value of $(R_s)_g$ when it did not change significantly with an appreciable increase in g. The required computer data were:

Input constants:

$$\dot{k} = 1.38 \times 10^{-16}$$
$$T = 1000$$
$$\sigma = 247.7$$
$$\rho = 1.92$$
$$C_e = 6.92 \times 10^{12}$$
$$C_2 = 1.1 \times 10^{12}$$
$$C_3 = 1.78 \times 10^{11}$$
$$m_1 = 4.30 \times 10^{-23}$$
$$m_2 = 8.60 \times 10^{-23}$$
$$m_3 = 12.90 \times 10^{-23}$$

Input parameters: S, S_2, S_3, S_α, C_D, Ak_g^r [in present work, $(\alpha_g)_1 = (\alpha_g)_2 = (\alpha_g)_3 = 1$]

Input variable: g

Computer output: $(R_s)_g$

where S is the supersaturation of the monomer with respect to condensed phase, S_2 and S_3 are the supersaturations of the dimer and trimer with respect to the dimer and trimer present at equilibrium, S_α is the supersaturation of LiX (Equation 90 of reference 1), $\underline{S}$ is the complex supersaturation (Equation 91 of reference 1), and C_D is the concentration of X in equilibrium with bulk LiF (1). (The nomenclature is given in detail in Section IX of reference 1.)

An assortment of input parameters was used, but the influence of specific parameters remains largely uncertain because of interaction between the parameters.

Results are given in Figures 4 to 6 and the effect of Ak_g^r* is summarized in Figure 7. Dashed lines indicate that g is less than 20 and the liquid-drop theory would not be expected to be applicable. The arrows in the figures

---

* Ak_g^r is the specific rate constant for the reaction of the P_g cluster with D to form the P_{g-1} cluster, A, and B.

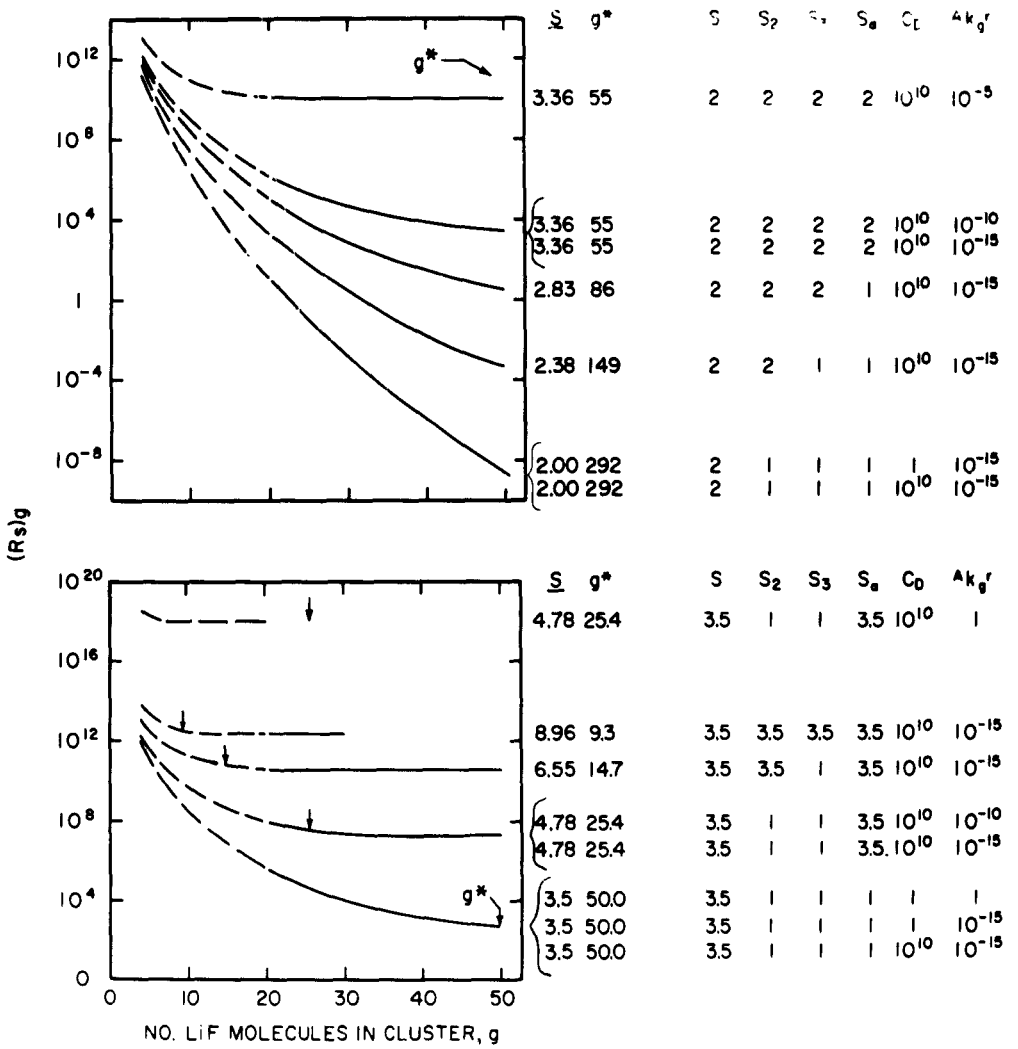

FIGURE 4. NUCLEATION FROM THE COMPLEX Li-F-X SYSTEM

S = 2 AND 3.5 T = 1000°K

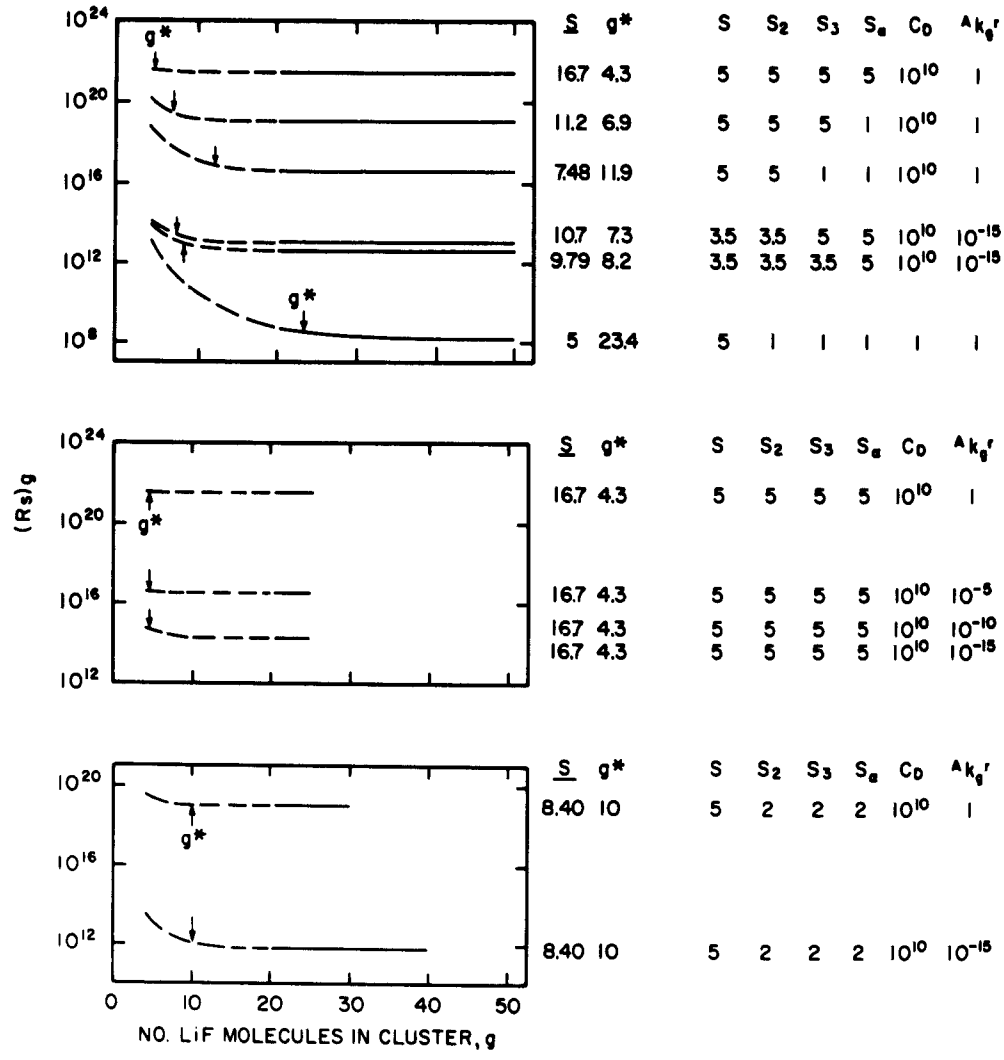

FIGURE 5. NUCLEATION FROM THE COMPLEX Li-F-X SYSTEM

S = 5 T = 1000°K

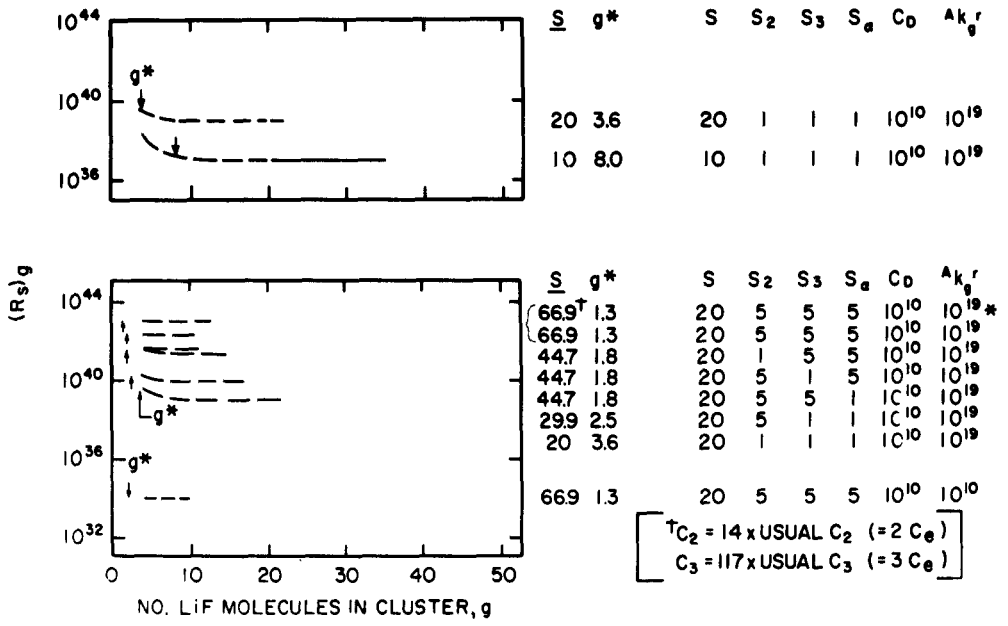

FIGURE 6. NUCLEATION FROM THE COMPLEX Li-F-X SYSTEM

S = 10 AND 20 T = 1000°K

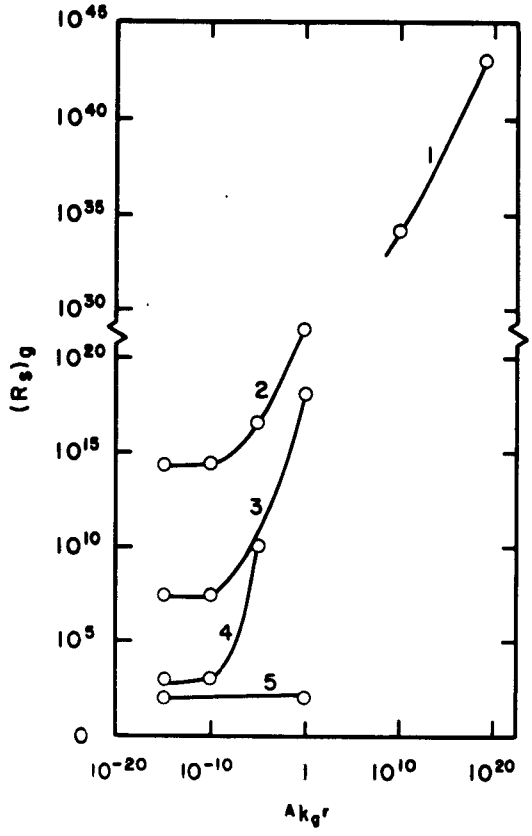

	S	S	S_2	S_3	S_4	C_D
1.	66.9	20	5	5	5	10^{10}
2.	16.7	5	5	5	5	10^{10}
3.	4.78	3.5	1	1	3.5	10^{10}
4.	3.36	2	2	2	2	10^{10}
5.	4.78	3.5	1	1	3.5	1

FIGURE 7. EFFECT OF Ak_gr ON NUCLEATION FROM THE COMPLEX Li-F-X SYSTEM AT 1000°K

indicate the location of g*. $(R_s)_g$ decreased as g increased and usually leveled at a steady value, which was taken as $(R_s)_{complex}$. (A similar variation occurred in the previously reported computation of nucleation from an equilibrated monomer-dimer system and was discussed there.) $(R_s)_g$ leveled for a value of g greater than the classical liquid-drop g* and was independent of Ak_g^r if Ak_g^r was about 10^{-10} or less. However, this leveling occurred for a g less than g* when Ak_g^r was large (e.g., 1 or 10^{-5}). The latter situation implies that nucleation involves clusters which contain fewer molecules than the classical liquid-drop nucleus.

The value of $(R_s)_{complex}$ increased as $\underline{S}$ increased except that a low value of C_D could decrease $(R_s)_{complex}$ despite a higher $\underline{S}$ (see Figure 7, bottom curve).

A closer examination of the present results might reveal other trends, but this was not done for the present report.

Condensation Kinetics of B_2O_3 and LiF (Constant Volume)

The rates of condensation of B_2O_3 and LiF liquids were computed by the previously reported modified theory (pp. 65-69 of reference 1) which assumed:

a. Modified liquid-drop nucleation (3) of liquid particles
b. Collision-frequency growth of liquid particles
c. Particle temperature equal to vapor temperature
d. Accommodation coefficient of 1

The present brief results are exactly comparable to the previously reported results for water condensation. Input data are given in Table I. Inert gas pressure ranged from 2.6 to 8.3 atm in most of the present calculations.

Results for B_2O_3 are given in Figures 8 and 9 and for LiF in Figures 10 to 13. Figure 14 summarizes the times required for 50% of condensation. The effect of inert gas will be noted; for example, with LiF at 2000°K, decreasing the inert gas from 5.5 to 0.55 atm decreased the time required for 50% condensation about 25%, but a further decrease had only a minor influence.

TABLE I

COMPUTER INPUT DATA FOR B_2O_3 AND LiF

	B_2O_3 [a, b]			LiF [a, b]		
T, °K	1,000	1,700	2,300	1,000	1,521	2,000
ΔH_l	84,500	79,600	75,700	56,550	53,400	50,260
A	18,500	17,450	16,580	12,400	11,670	11,000
B	29.816	28.989	28.540	28.240	27.680	27.251
ρ_l	1.55	1.47	1.43	1.92	1.57	1.37
σ_l	73.0	98.0	117	248.0	198.0	149.0
$C_{e,l}$	2.070×10^{8}	3.110×10^{13}	9.330×10^{17}	6.920×10^{12}	6.700×10^{16}	2.820×10^{18}
ρ_z, atm	2.6	4.6	8.3	2.6	4.2	5.5

[a] $m_{B_2O_3} = 1.16 \times 10^{-23}$ g; $m_{LiF} = 4.31 \times 10^{-23}$ g

[b] $c_z = 2.01 \times 10^{19}$ molecules/cm^3

$\beta_z = 8.0$

$\beta_l = 30.0$

$\beta_v = 21.9$

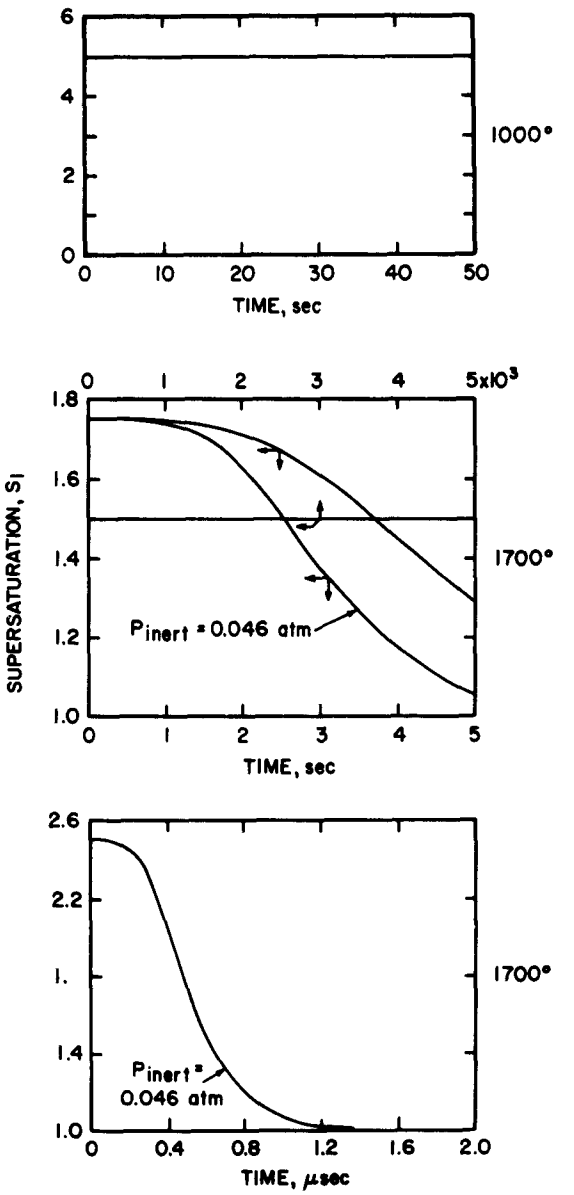

FIGURE 8. CONDENSATION OF B_2O_3 LIQUID AT 1000 AND 1700°K

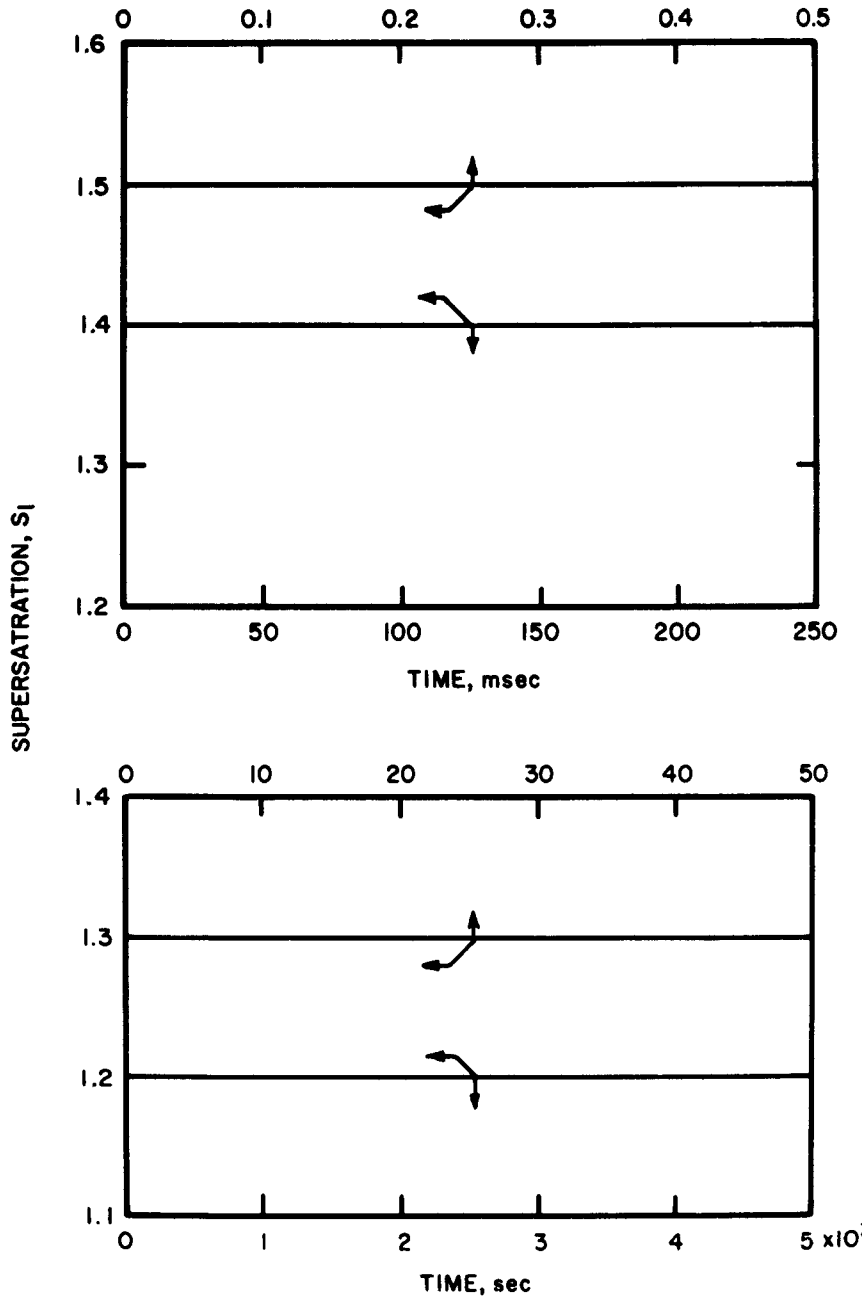

FIGURE 9. CONDENSATION OF B_2O_3 LIQUID AT 2300°K

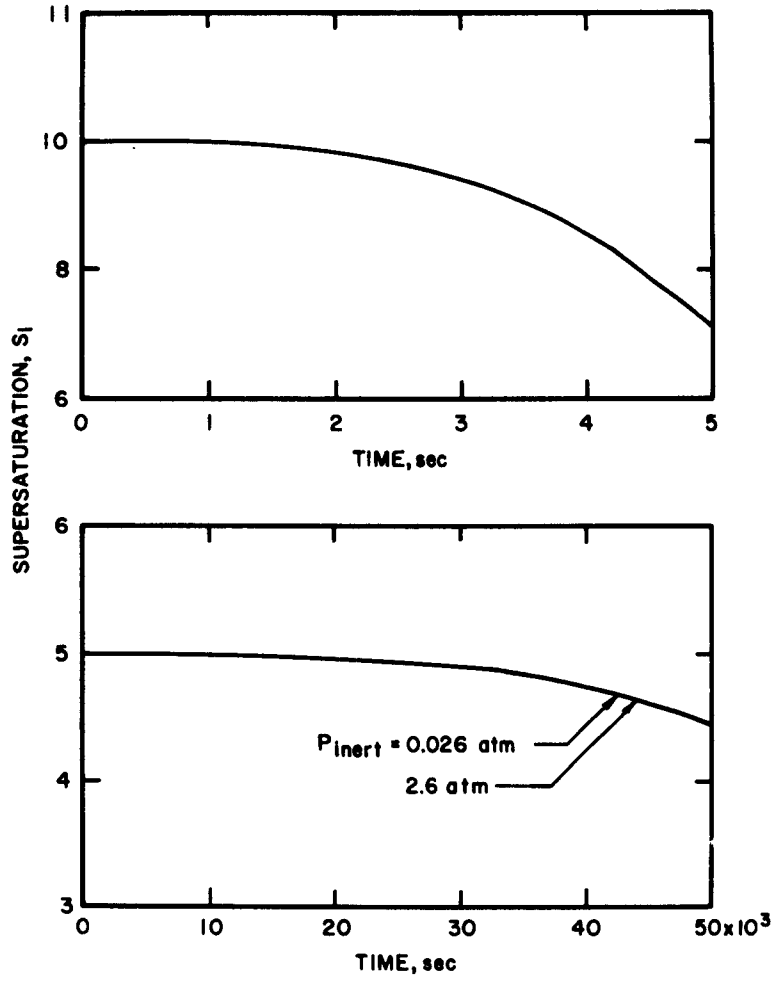

FIGURE 10. CONDENSATION OF LiF LIQUID AT 1000°K

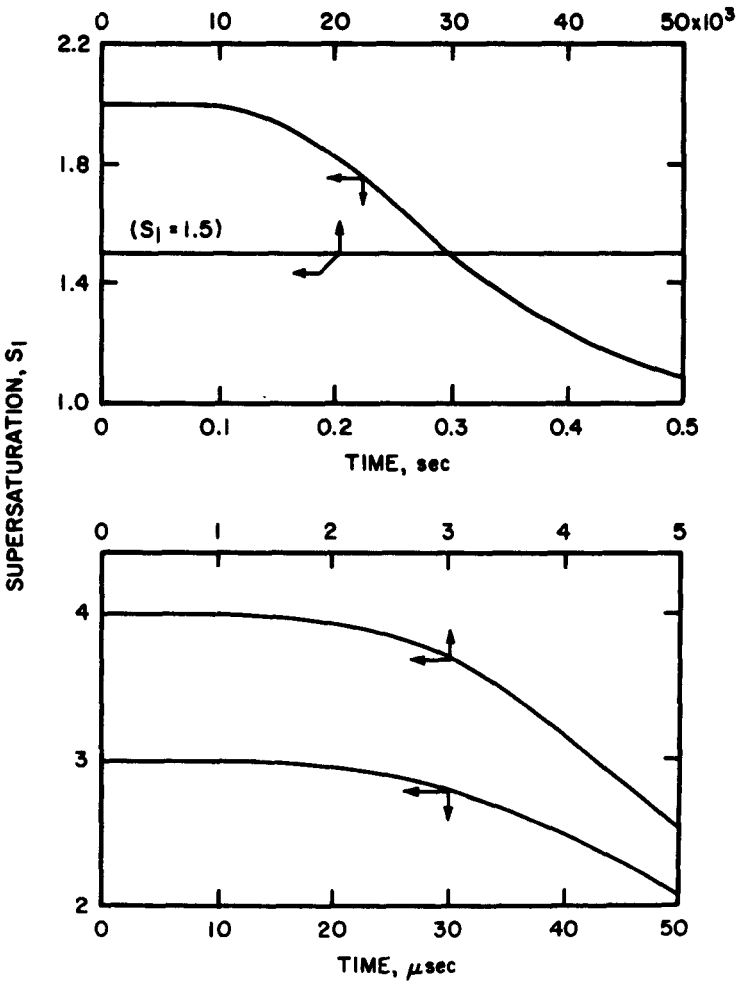

FIGURE 11. CONDENSATION OF LiF LIQUID AT 1521°K

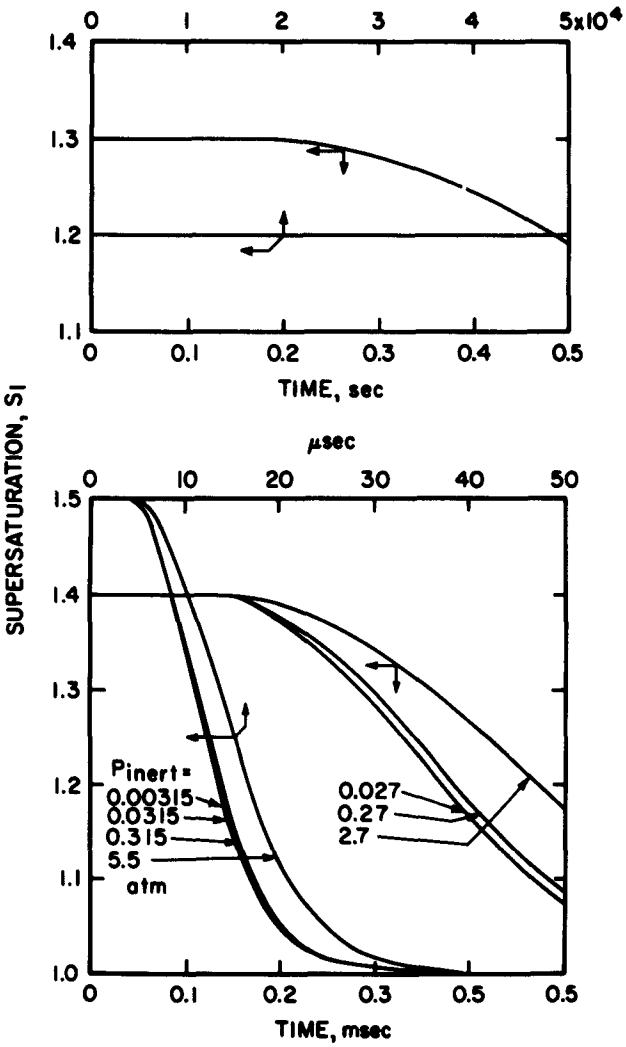

FIGURE 12. CONDENSATION OF LiF LIQUID AT 2000°K

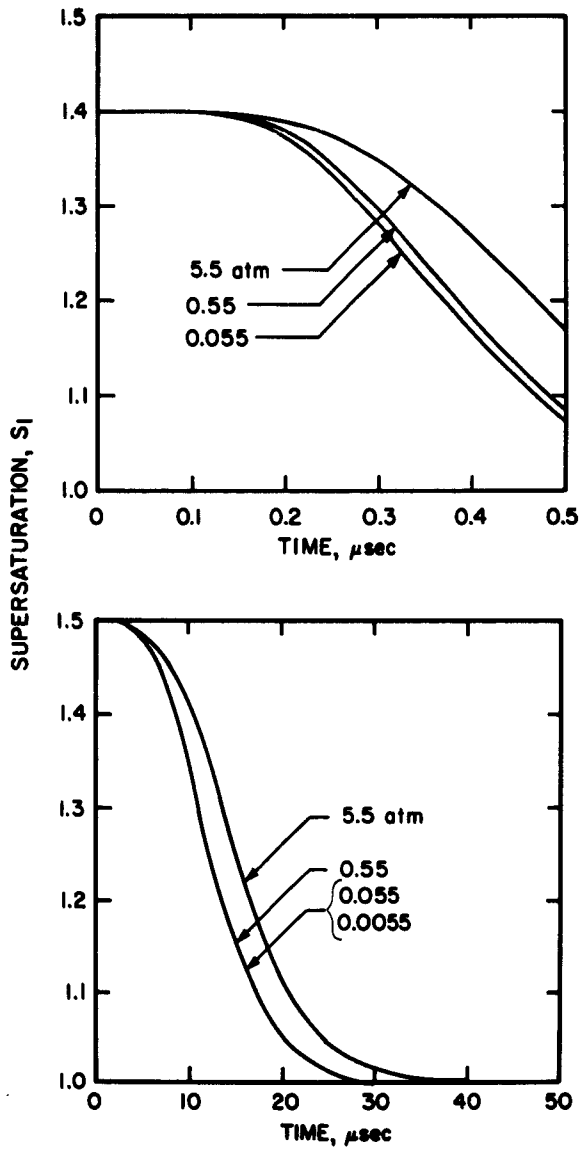

FIGURE 13. EFFECT OF INERT GAS ON RATE OF CONDENSATION OF LiF LIQUID AT 1000°K

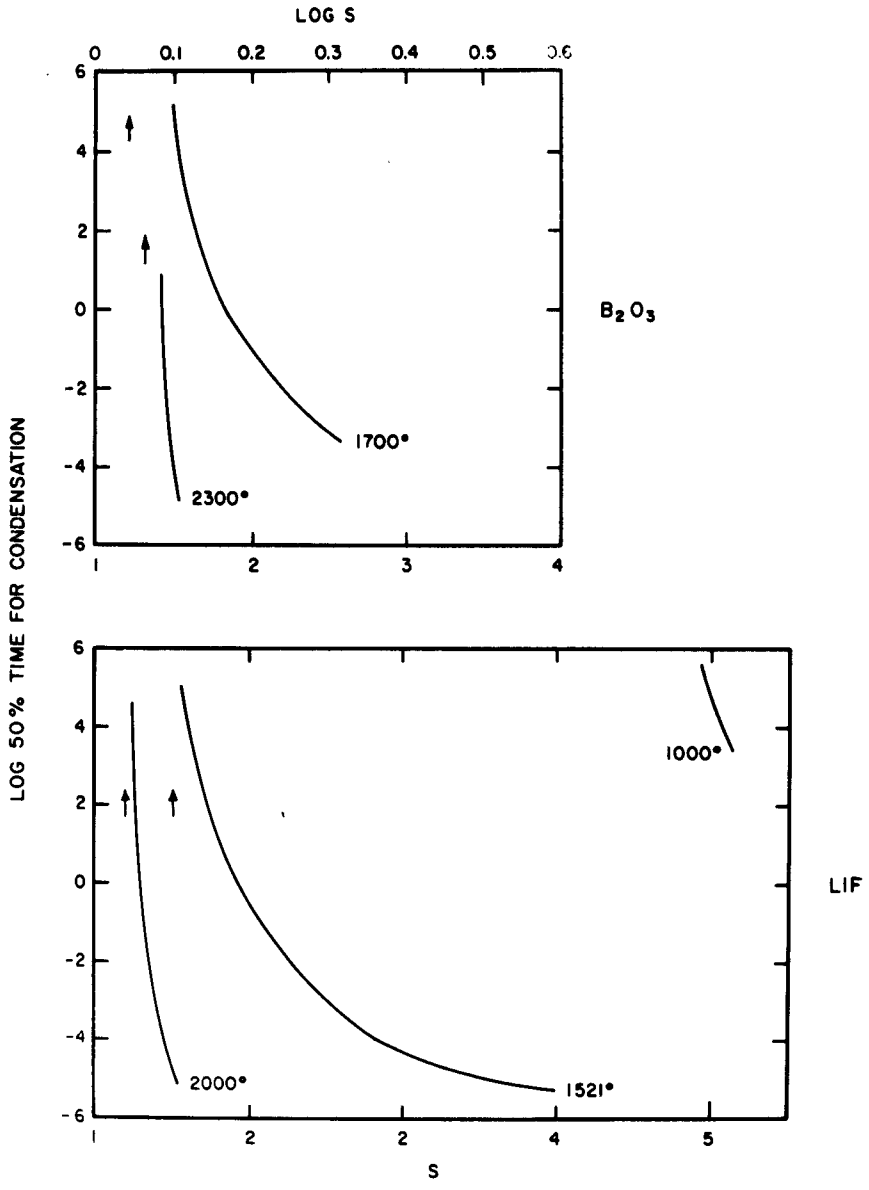

FIGURE 14. SUMMARY OF 50% TIMES FOR CONDENSATION OF B_2O_3 AND LiF LIQUIDS

TIME IS IN MICROSECONDS

Condensation in Nozzles (Variable Volume)

The 50% times for condensation of B_2O_3 and LiF may be incorporated into the previously reported plots (Figures 39 and 40 of reference 1), which describe the condensation conditions obtained in certain wind-tunnel and rocket-nozzle cases. The 50% times for case A in the B-O-H systems and for case B in the Li-F systems are uncertain to perhaps 20% since the pressures of "inert gas" in the nozzle cases were appreciably different from the pressures used to obtain the 50% times.

Results for H_2O (from data given in reference 1) are given in Figure 15 and for B-O-H and Li-F propellants in Figure 16.

With H_2O the 50% time for condensation in the selected cases is about 1000-fold greater than the local residence time, and a problem in condensation may be anticipated. With B_2O_3 the 50% times rapidly decrease to become less than the local residence times in the two cases, and no problems are anticipated. With LiF no problem is expected for case B, but a condensation problem may be expected for case A.

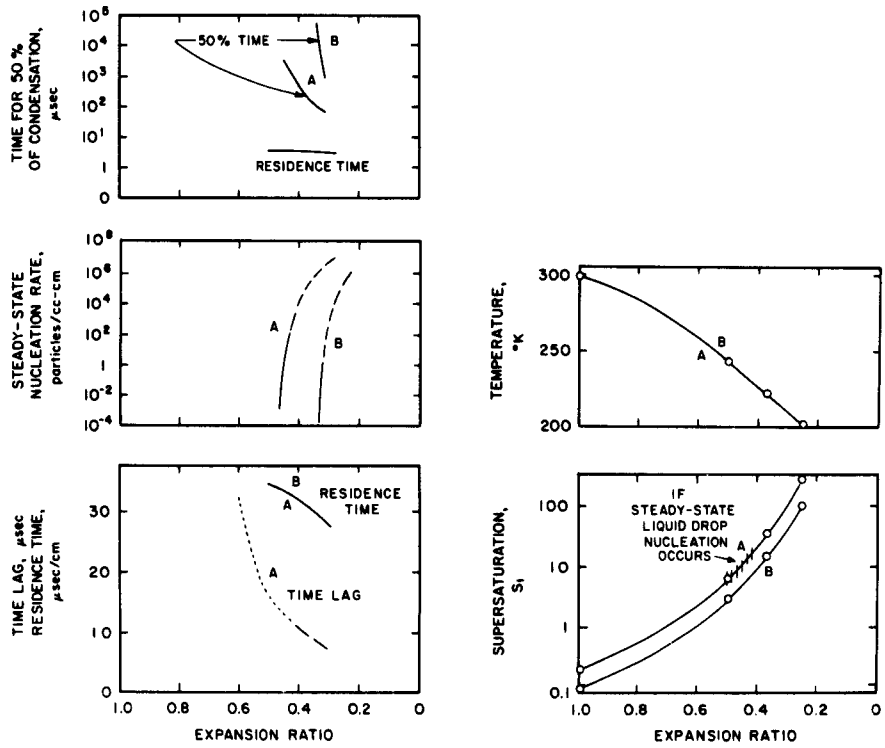

FIGURE 15. CONDENSATION OF H_2O IN WIND TUNNEL

INITIAL CONDITIONS

A. N_2 + 0.0061 H_2O (SAT. AT 273°K), 1 atm, 298°K

B. N_2 + 0.0028 H_2O (SAT. AT 263°K), 1 atm, 298°K

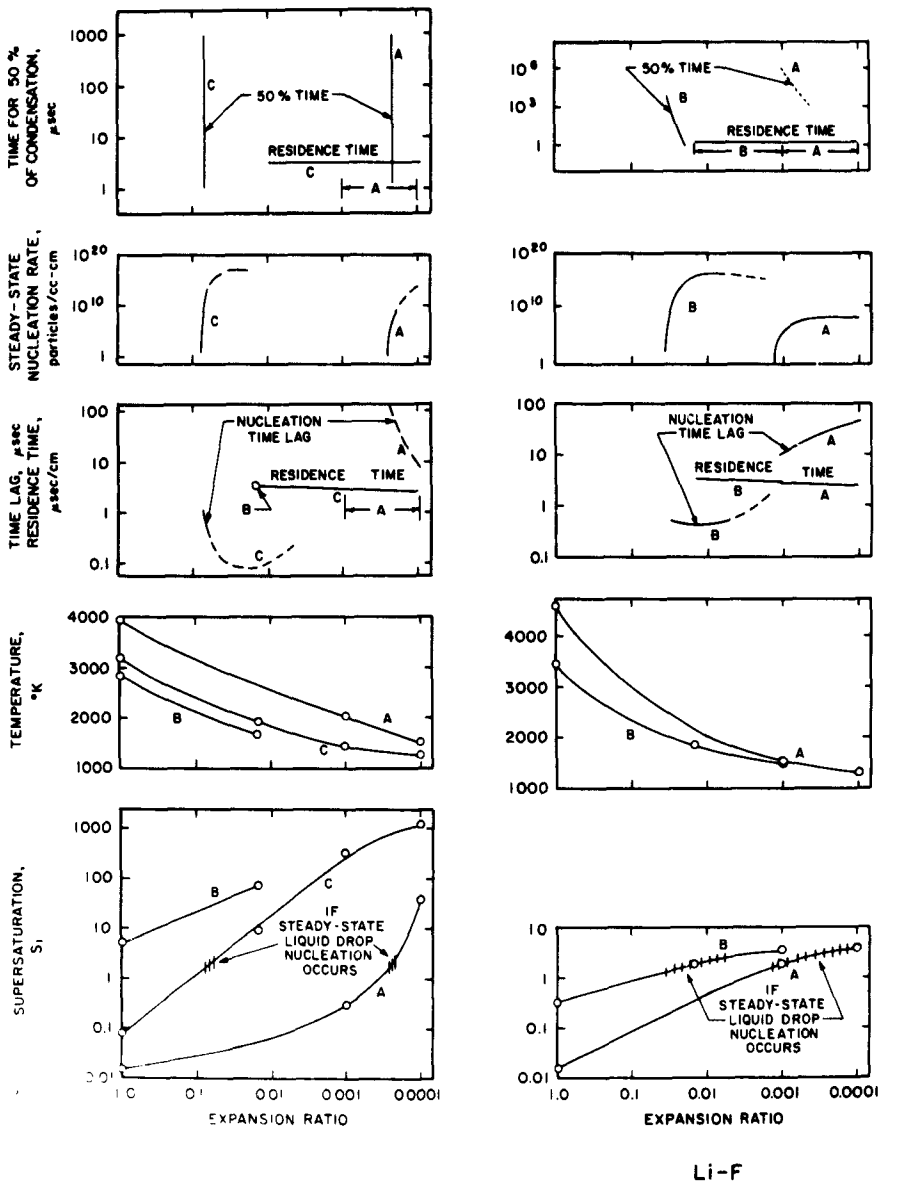

FIGURE 16. CONDENSATION OF B_2O_3 AND LiF IN ROCKET NOZZLE

INITIAL CONDITIONS

B-O-H:

A. 3922°K, 68 atm (OBTAINED FROM B_5H_9 + 2.1 N_2O_4 AT 298°K)

B. 2843°K, 68 atm (OBTAINED FROM B_5H_9 + 3.75 H_2O_2 AT 298°K)

C. 3175°K, 68 atm (OBTAINED FROM B_5H_9 + 5 H_2O_2 AT 298°K)

Li-F:

A. 4598°K, 68 atm (OBTAINED FROM LiH + 0.5 N_2F_4 AT 298°K)

B. 3439°K, 68 atm (OBTAINED FROM LiH + 0.25 N_2F_4 AT 298°K)

EXPERIMENT

The experimental investigation of the kinetics of condensation of water from a water vapor-inert gas mixture was continued to obtain data to compare with the theoretical results.

The present experimental results are believed to be meaningful, although the lack of time did not permit doing several planned variations in the experimental technique as a check on the present experimental technique.

Interpretation of the results is incomplete. Although the writer plans to attempt elsewhere a quantitative interpretation of the results, the publication date of subsequent work is uncertain. Therefore, representative examples of the raw data for pressure during condensation in the present cloud chamber are given in the Appendix for the consideration of other workers.

Equipment and Technique

The equipment and technique generally followed the description in the previous report (1). However, the results using subatmospheric pressures in the cloud chamber before expansion were obtained by operating the thermostated filter at the usual temperature and then slowly evacuating the chamber to 1/2 or 1/3 atm before expansion. Operation at elevated chamber pressure required replacing the glass parts of the pretreatment apparatus with metal parts and using a 3/4-inch plate-glass top on the expansion chamber. A Bourdon-type pressure gauge reading to 1/40 psi was connected to the gas-water inlet line to the chamber. Inert gas was passed through the chamber at slightly above the desired elevated pressure by a throttling valve at the exit line on the chamber. The valve on the inert-gas cylinder was then closed and the throttling exit valve closed when the Bourdon gauge read the desired pressure. Considerable care was taken to ensure that the chamber pressure never became excessive, for the relieving of a local excess pressure might lead to anomalous condensation in the system. Several condensations at unexpectedly low expansion ratios are thought to be due to this effect.

The heat-capacity ratio for a mixture of gases A and B is given by

$$\frac{1}{\gamma_{mix} - 1} = \left(\frac{1}{\gamma_A - 1}\right)\frac{p_A}{P} + \left(\frac{1}{\gamma_B - 1}\right)\frac{p_B}{P}$$

where γ_{mix} is the ratio for the mixture, γ_A and γ_B apply to pure A and pure B, p_A and p_B are the partial pressures of A and B in the mixture, and P is the total pressure of the mixture. The heat-capacity ratios of systems of interest were taken as:

$$\gamma_{H_2O} = 1.330$$
$$\gamma_{N_2} = 1.404$$
$$\gamma_{Ar} = 1.660$$
$$\gamma_{He} = 1.670$$

and were assumed independent of temperature.

Results

It is most instructive to convert the experimental pressure-time curves to supersaturation-time curves. Figure 17 schematically shows the supersaturation-time curves obtained in the present cloud chamber when dry and wet inert gas were expanded. The piston rapidly dropped after falling off the cam, thereby rapidly increasing the supersaturation in the vapor. After the piston hit bottom it bounced twice, thereby abruptly decreasing the supersaturation twice. Heat conduction into the cooled vapor from the "hot" wall then decreased the supersaturation as time continued to increase. Figure 18 shows actual experimental results derived by the adiabatic expansion law from the condensation run presented as Figure 47 in reference 1, and assuming no condensation.

The pressure dependence upon time during piston bounce corresponded approximately to

$$P_t = 569 - 3.5\,(2 - t)^2 \qquad 0 \leq t \leq 4$$
$$= 564 - 5.6\,(4.4 - t)^2 \qquad 4 < t \leq 5.8$$

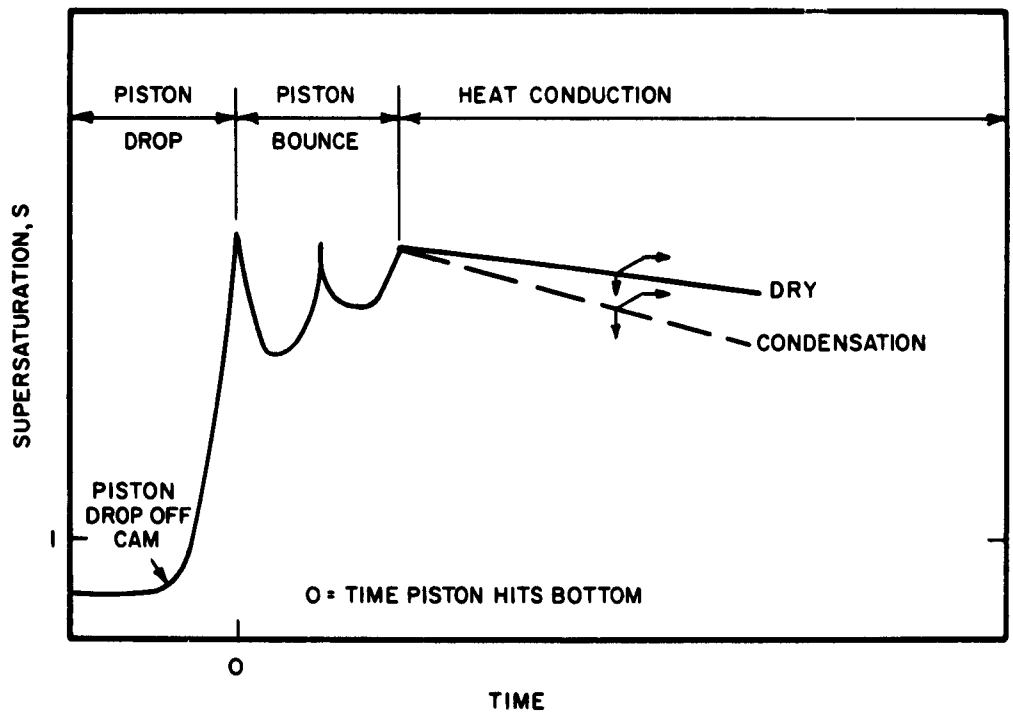

FIGURE 17. SCHEMATIC DIAGRAM OF SUPERSATURATION DURING OPERATION OF CLOUD CHAMBER

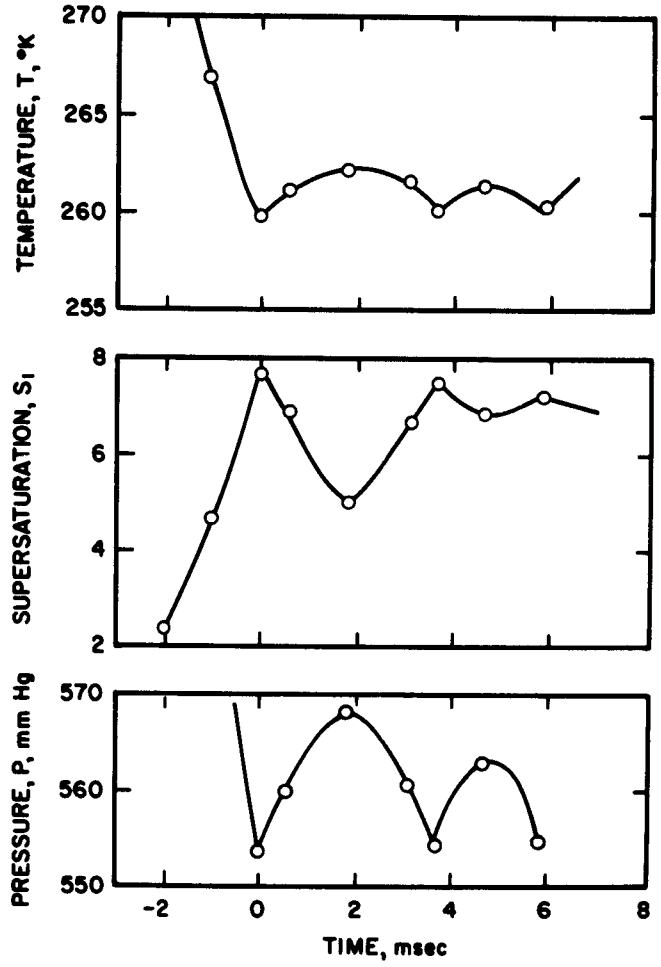

FIGURE 18. PRESSURE, SUPERSATURATION, AND TEMPERATURE DURING PISTON BOUNCE ASSUMING NO CONDENSATION

CONDENSATION RUN SAME AS FIGURE 47 IN REFERENCE I.

ZERO ON TIME SCALE INDICATES PISTON STRIKING BOTTOM

Figure 18 thus presents the situation (S and T) for condensation in that run. Although the nominal supersaturation in the system was 7.7, the vapor initially was in a very time-dependent system and at first only spent 1 msec above a supersaturation of 7.

From a condensation viewpoint, therefore, the vapor is in a state which varies with time (a) abruptly during the first 5 or so msec because of piston motion and bounce and (b) moderately during the remaining time because of heat conduction. In view of the time-dependent situation and particularly of the error in supersaturation in the present work, the quantitative usefulness of the present results is perhaps doubtful. However, the experimental errors in the present work are believed to be about the smallest absolute errors obtainable in a cloud chamber without going to exceedingly expensive equipment. Although this absolute error is still a burdensome relative error from the viewpoint of supersaturation, it is of interest to analyze the present results to determine the general usefulness of an expansion chamber for condensation experiments.

"Memory" Effect

As noted previously, a memory effect was encountered with "used" gas, where wet gas was purposefully overexpanded to give a dense visible mist and then recompressed, held recompressed for several minutes, and then again expanded. The intensity of the scattered light was reduced to the background level in about 1 sec or less after recompression, suggesting that the particles in the mist had evaporated.

Typical results showing the effect of hold time after recompression are given in Figure 19. The amount of scattered light after the re-expansion seemingly should depend primarily upon the expansion ratio of the re-expansion, i. e., upon the amount of water which condensed during the re-expansion. Since this ratio was held constant in Figure 19, the observed variation in the maximum scattering is perhaps due to a difference in the size distribution of the particles appearing after the second expansion.

Semiquantitative Interpretation

As noted previously (1), upper envelopes to the scattering-time curves obtained with fresh vapor were drawn and the times required to achieve 50% of the maximum scattering intensity were noted. The initial supersaturation and temperature (i. e., after expansion but before condensation)

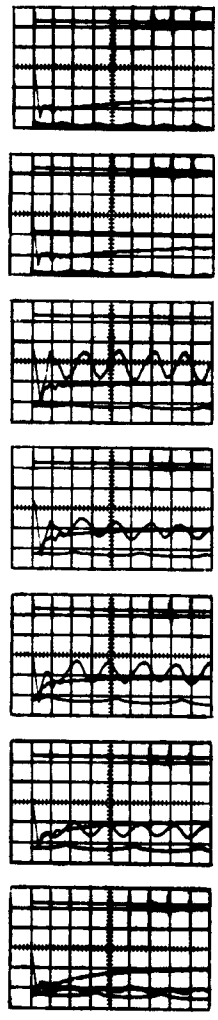

PREVIOUS EXPANSION RATIO	T_0, °K	S_1	RECOMPRESSED HOLD TIME, min
		(DRY)	
		(NONE)	
1.356	239.6	37	1
1.356	239.6	37	2
1.553	219.4	250	2
1.553	219.4	250	5
1.553	219.4	250	10

FIGURE 19. "MEMORY" EFFECT IN CLOUD CHAMBER

INITIAL CONDITIONS	SUBSEQUENT EXPANSION
THERMOSTAT TEMPERATURE, 19.0°C	EXPANSION RATIO, 1.158
CHAMBER TEMPERATURE, 19.0°C	SUPERSATURATION, 3.53
CHAMBER PRESSURE, 761 mm Hg	TEMPERATURE, 265.5°C

of each run were then plotted with the 50% time noted. Results are given in Figures 20 to 23, where the actual pressures in the chamber after expansion were 0.18, 0.25-0.26, 0.51-0.75, and 2.2 atm* respectively, with the lower value in each case applying to the lower temperature in the particular figure. Superimposed on these figures are the theoretical values for the 50% time when the partial pressure of the inert gas was 0.526 atm (400 mm Hg).

The approximate supersaturations required at a certain temperature to give 50% condensation in, say, 10 msec can be extracted from the above figures and plotted against the actual partial pressure of inert gas in the condensing system. Figure 24 is such a plot and shows the experimental effect of the partial pressure of the argon in the system on the rate of condensation as taken from the above scattering curves. The theoretical values for 0.526 atm are included.

Figure 24 therefore summarizes the present experimental and theoretical results. The close agreement between theory and experiment is satisfying but is undoubtedly largely coincidental.** The experimental value at 2.2 atm is somewhat lower than expected, but the high-pressure data were measured in haste at the end of the contract and therefore may be incorrect. Additional theoretical condensation curves with other partial pressures of argon will be calculated to check this apparent agreement between theory and the semi-quantitative interpretation of the present light-scattering experiments.

Quantitative Interpretation

Quantitative interpretation of the experimental pressure-time curves requires conversion of the pressure-time curve to a supersaturation-time curve via a theoretical calculation of the corresponding temperature-time curve.

Calculation of this temperature during condensation requires taking into account (a) heat conduction into the chamber from the walls and (b) the nonisentropic nature of the condensation.

---

* The nominal chamber pressures before expansion were 0.33, 0.5, 1.0, and 3 atm, respectively.

** The experimental points used to draw the experimental lines in Figure 24 were taken by crude visual inspection from Figures 20 to 23 but were taken before the theoretical point was known.

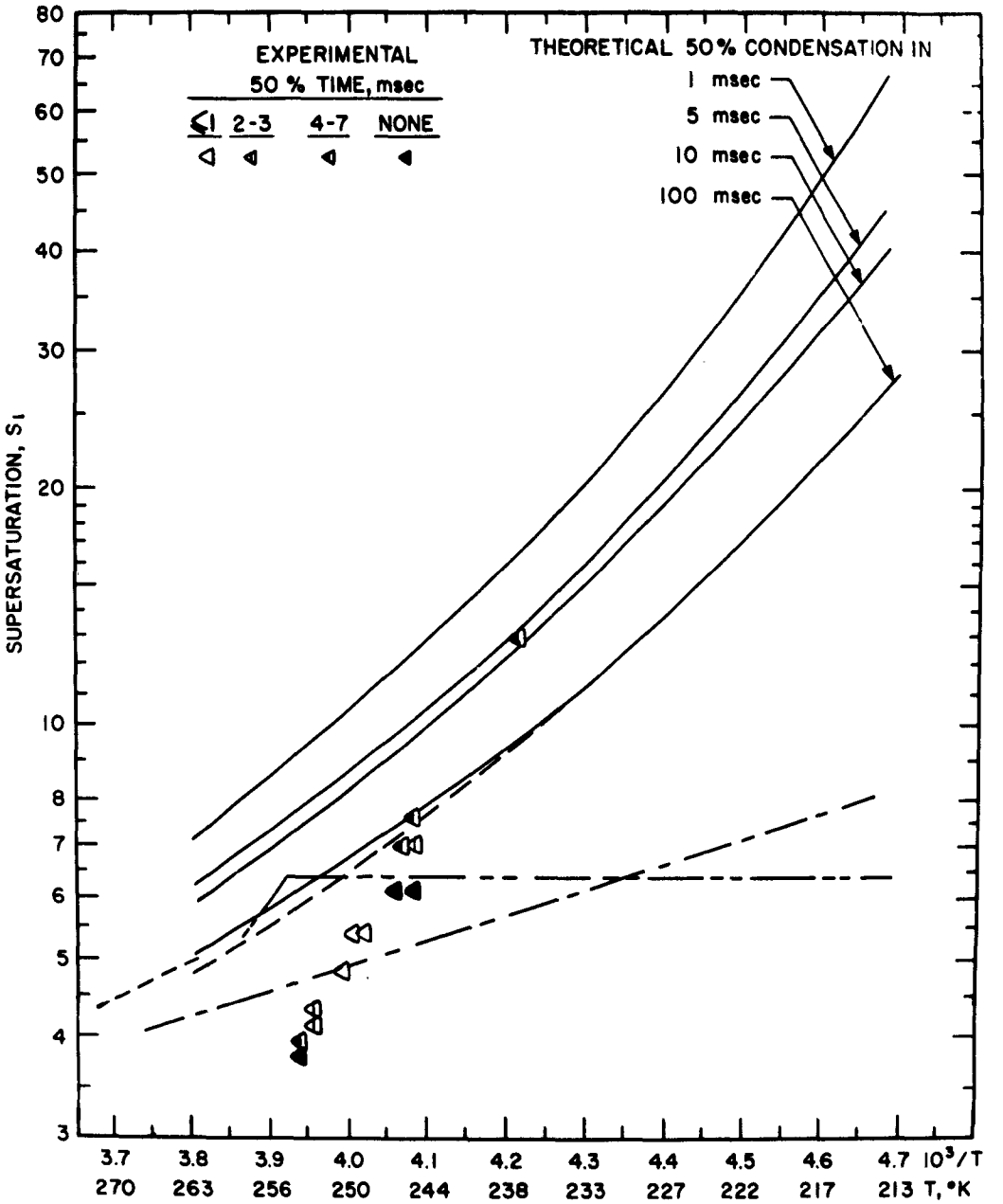

FIGURE 20. SEMIQUANTITATIVE COMPARISON OF THEORY AND EXPERIMENT FOR CONDENSATION OF WATER WITH 0.18 ATM INERT GAS

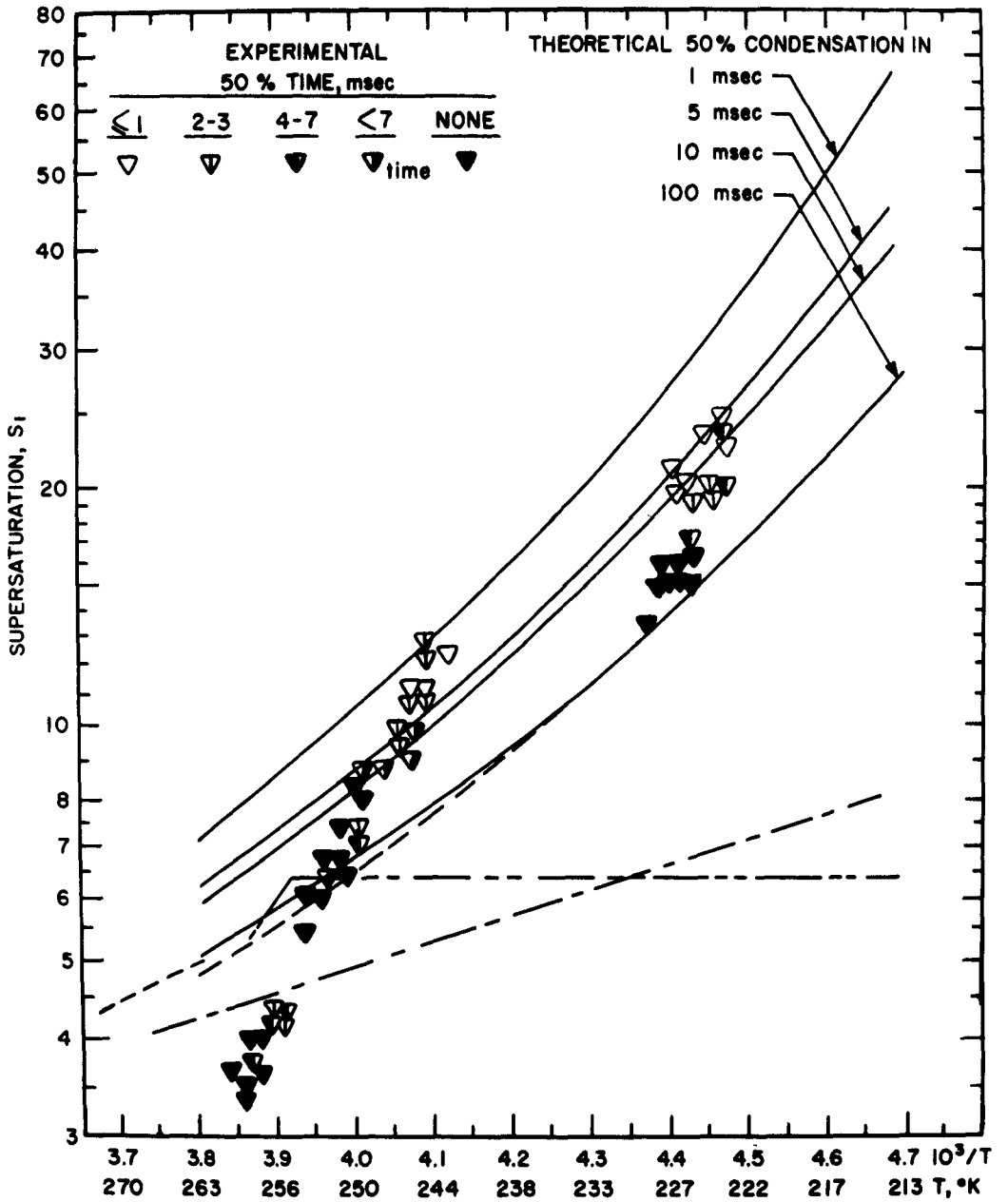

FIGURE 21. SEMIQUANTITATIVE COMPARISON OF THEORY AND EXPERIMENT FOR CONDENSATION OF WATER WITH 0.26 TO 0.31 ATM INERT GAS

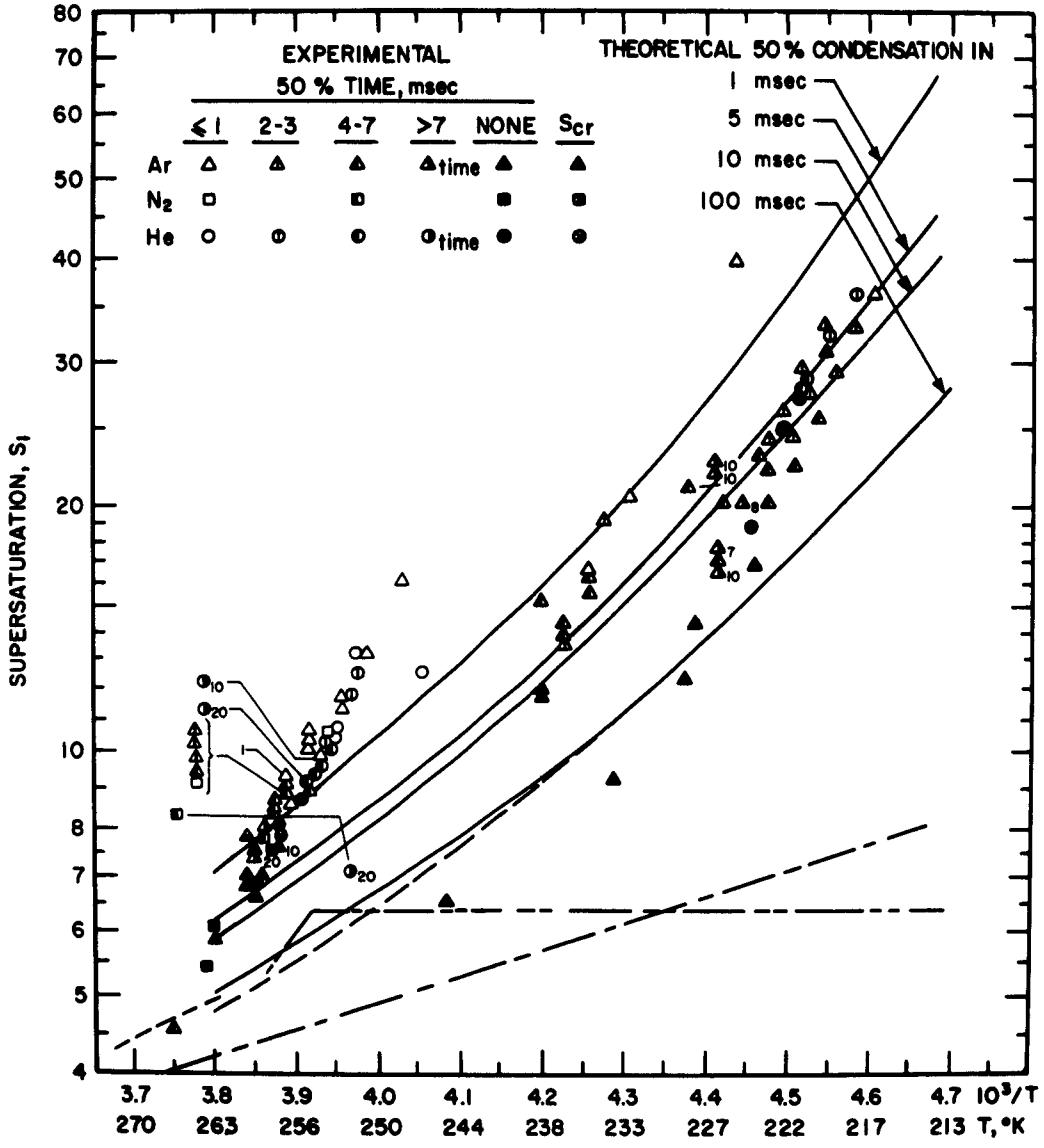

FIGURE 22. SEMIQUANTITATIVE COMPARISON OF THEORY AND EXPERIMENT FOR CONDENSATION OF WATER WITH 0.52 TO 0.75 ATM INERT GAS

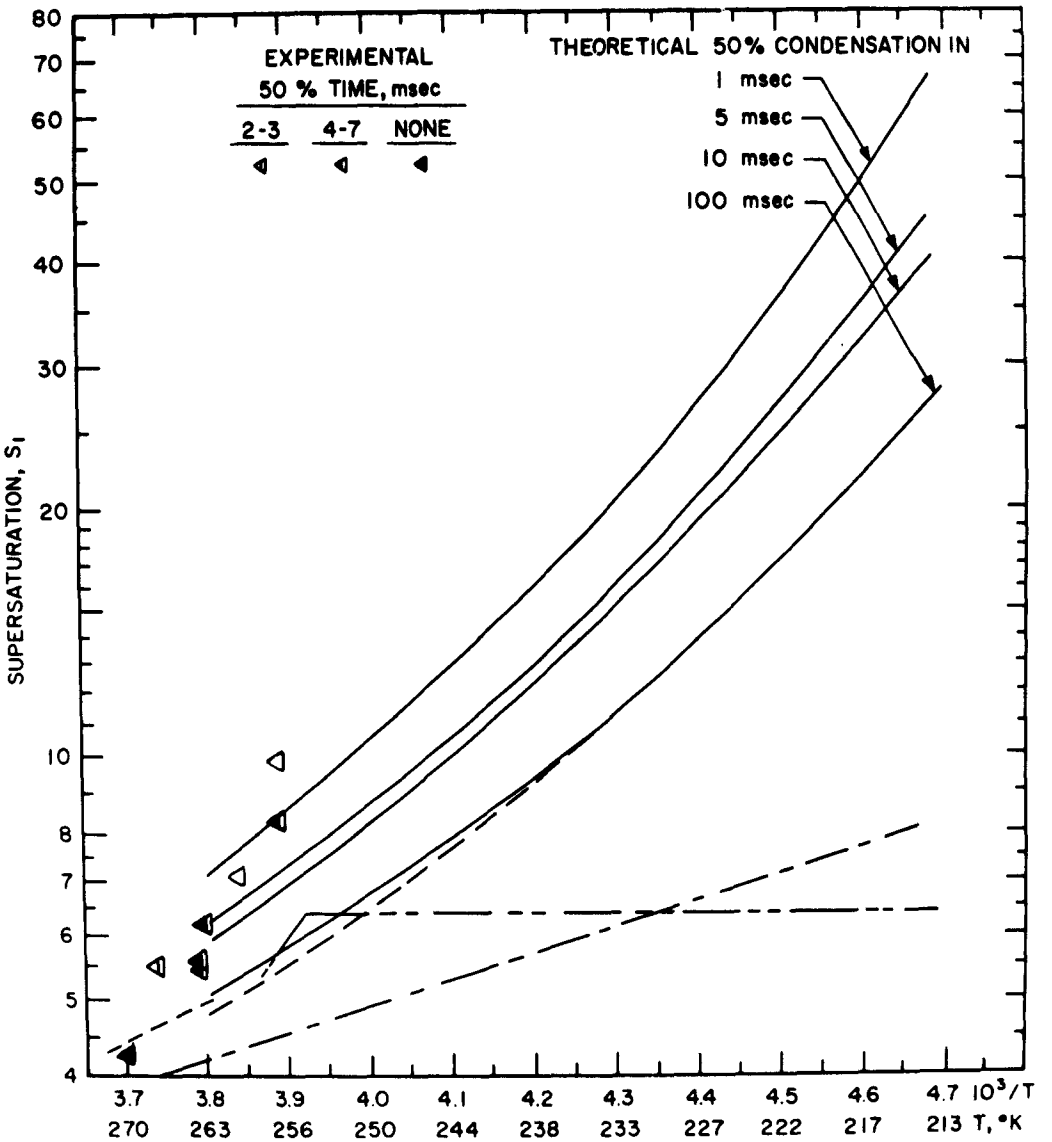

FIGURE 23. SEMIQUANTITATIVE COMPARISON OF THEORY AND EXPERIMENT FOR CONDENSATION OF WATER WITH 2.2 ATM INERT GAS

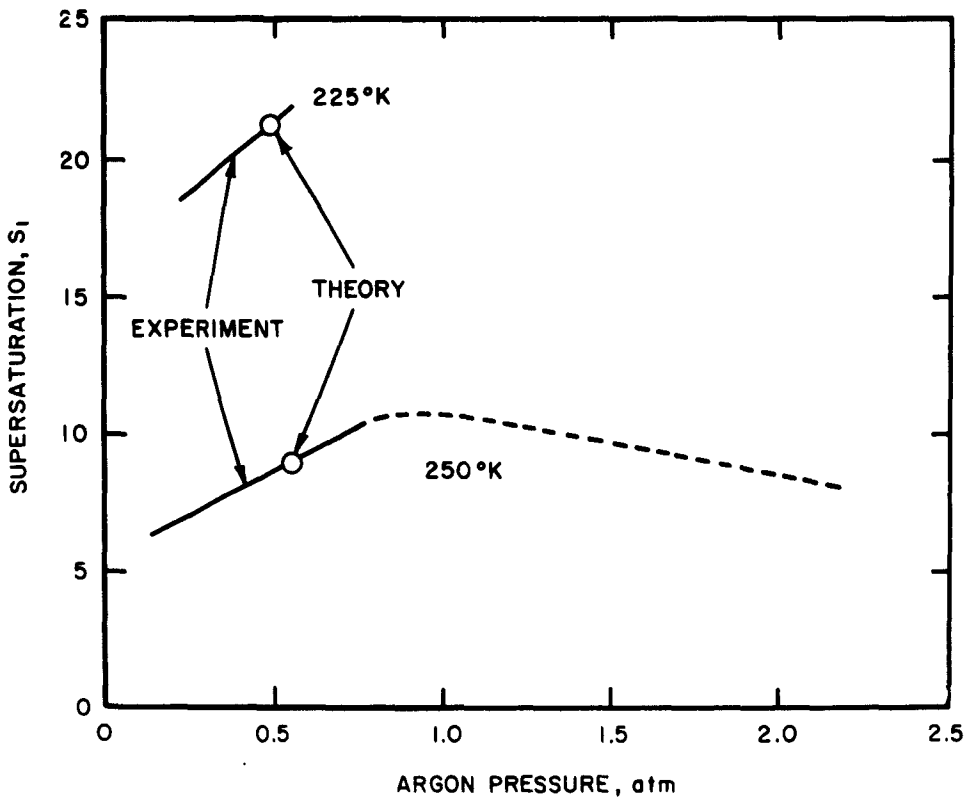

FIGURE 24. SUMMARY OF CONDENSATION COMPARISONS — EFFECT OF INERT GAS

Heat Conduction into Chamber. Immediately after expansion the surfaces of the chamber walls, piezoelectric gauge, etc. are at a temperature appreciably above the temperature of the expanded gas. Heat therefore tends to be conducted into the gas layer adjacent to these hot surfaces. This gas layer tends to expand, thereby compressing the remaining bulk gas.

If this compression of the bulk gas is adiabatic and is assumed to be reversible (thus is assumed to be isentropic), the pressure and temperature of the bulk gas at time t are respectively given by heat-conduction theory as

$$P_t - P_o = k_1 t^{1/2} = 1.14\gamma \frac{P'A}{T_o V} (T' - T_o)\, h t^{1/2} \tag{1}$$

$$T_t - T_o = k_2 t^{1/2} = 1.14\,(\gamma - 1)\,\frac{A}{V}\,(T' - T_o)\, h t^{1/2}$$

However, the volume change may be calculated without using the assumption of reversibility to give

$$V_t - V_o = k_3 t^{1/2} = -1.14A\,\frac{(T' - T_o)}{T_o}\, h t^{1/2} \tag{2}$$

and finally, again assuming isentropy,

$$P_t - P_o = k_2 \frac{\gamma}{\gamma - 1}\,\frac{P'}{T_o}\, t^{1/2} \tag{3}$$

where

A = area of hot surfaces after expansion (area of expanded chamber + auxiliary equipment in chamber), cm^2

c = specific heat of gas, cal/g

h = $(\text{thermal diffusivity})^{1/2} = (K/c\rho)^{1/2}$

K = thermal conductivity of gas, cal/cm-sec-°K

P' = pressure before expansion, mm Hg

P_o = pressure immediately after expansion is completed, mm Hg

P_t = pressure at time t after expansion is completed, mm Hg

T' = temperature before expansion, °K

T_t, T_o = temperature at t = t and t = 0 after expansion, °K

t = time, sec

V_o = volume of chamber immediately after expansion, cm^3

V_t = "compressed" volume of chamber at time t after expansion is completed, cm^3

γ = heat-capacity ratio

ρ = density of gas, g/cm^3

Thus, P_t and T_t should vary as $t^{1/2}$ according to heat-conduction theory.

We are not acquainted with any experimental verification of this theory. Hazen (4) observed experimentally that the pressure in his cloud chamber varied essentially linearly with time when expansion times were about 100 msec or greater. He assumed a temperature equation of the type

$$T_t = Bt + Ct^{1/2}$$

and arrived at the final pressure equation

$$P' - P_o = 0.008\,(\theta)^{1/2}$$

where θ is the time involved in the expansion process. This equation agreed satisfactory with his measurements of the pressure after expansion when the expansion ratio was 1.125.

In the present work, for example, dry argon at 1-atm pressure was expanded with ratios up to 1.5 and with expansion times of 5 to 10 msec. Since the initial pressure after expansion can be adequately predicted by assuming adiabatic expansion (1), our approach therefore is necessarily different from Hazen's approach.

The experimental pressure-time curves in the present dry-expansion work were measured and converted to pressure-time curves (1). Figure 25 plots the results as pressure versus $t^{1/2}$, with the point at zero time calculated assuming adiabatic expansion. Experimental error in pressure is ±5 mm. Results could be adequately interpreted by the $P_t - t^{1/2}$ law. Plots of P_t versus $Bt + Ct^{1/2}$ showed appreciable curvature, and Hazen's approach was discarded. The slopes of the straight lines in Figure 25 are equal to k_1.

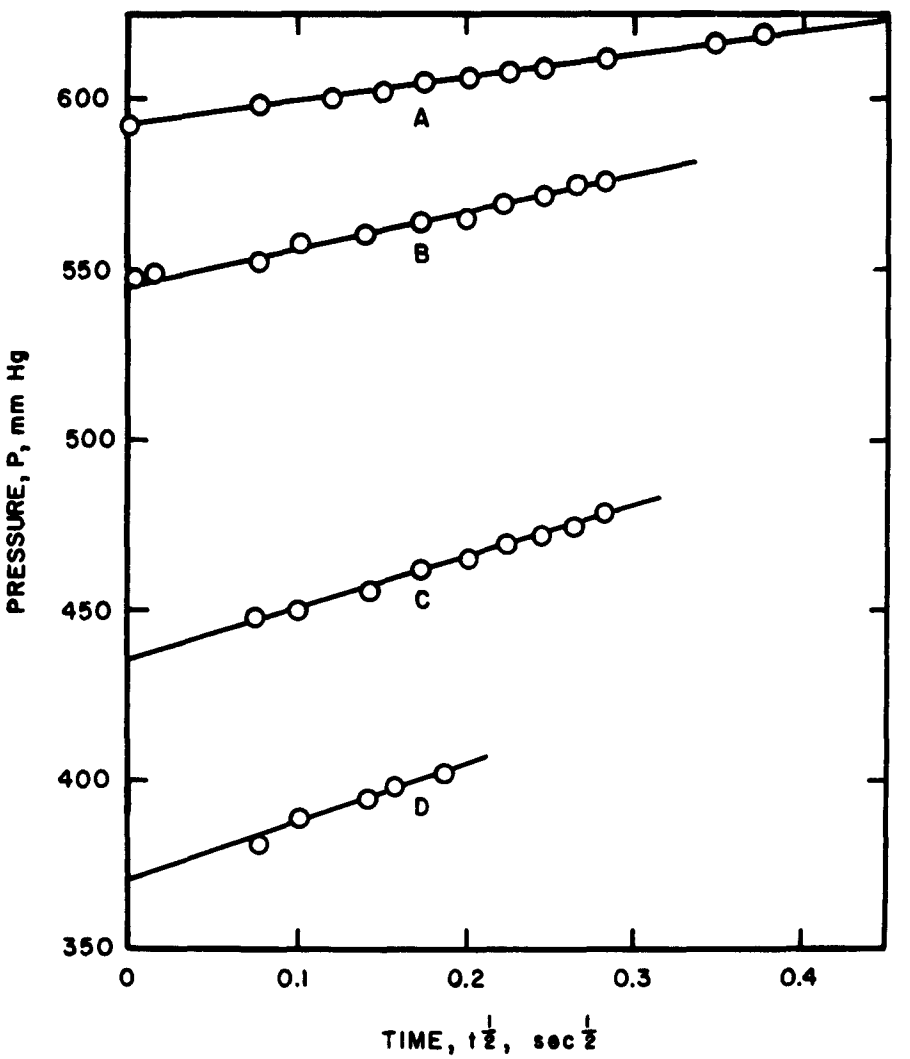

FIGURE 25. HEAT CONDUCTION FROM SURFACES INTO CLOUD CHAMBER

	A	B	C	D
INITIAL T, °K	293.3	293.3	293.8	296.0
P, mm Hg	760.8	767.0	760.2	761.0
EXPANSION RATIO	1.158	1.220	1.379	1.510
FINAL T, °K	266.1	259.5	237.6	225.6
P, mm Hg	591.4	551.3	446.3	384.0

Figure 26 plots the experimental values of k_1/P versus T' and also the experimental values of k_2 (calculated from Equations 1 and 3) versus expansion ratio. The theoretical variation of k_2 is included in Figure 26. This was calculated from Equation 3 using $k = 3.8 \times 10^{-5}$, $c = 0.12$, computed values of ρ assuming the ideal gas law, and the appropriate values for γ, A, and V. Figure 26 thus shows that the experimental heat conduction was somewhat greater than theory, but both the experimental and theoretical values of k_2 are somewhat uncertain. The experimental values of k_2 are used in later approximate calculations in this report.

Nonisentropic Nature of Condensation. Condensation inevitably is nonisentropic because of irreversibility. The temperature variation in a simple constant-volume, nonisentropic system can readily be calculated (viz., p. 66 of reference 1). However, the present cloud chamber, while nominally a constant-volume system, is actually a variable-volume system due to piston bounce and heat conduction. The effect on temperature of the time-dependent variation in volume must therefore be taken into account. Since the volume variation is not isentropic, the usual adiabatic calculation cannot be made.

The problem is to convert the experimental pressure at a time t to the supersaturation of the water vapor remaining in the chamber at this time. The problem can be resolved into (a) converting the experimental pressure to the number of moles of uncondensed water in the closed system, n, and the corresponding temperature and (b) converting n and T to supersaturation. The resulting supersaturation-time curve may then be compared to the theoretical supersaturation-time curve computed for the same initial supersaturation and temperature.

This calculation can be separated into a simple approximate approach, which neglects piston bounce and assumes heat conduction is isentropic, and a laborious exact approach, which incorporates piston bounce and makes no assumption about entropy.

1. Approximate Approach. The pressure in the chamber at any time t, P_t, is given by the ideal gas law as

$$P_t = \frac{(760)(0.08205)\, n\, T_t}{V_t} \tag{4}$$

where P_t is the pressure in mm, n is the total number of moles of gas in the system, T_t is temperature in °K, and V_t is the chamber volume in liters. For a water vapor-ice-argon mixture at constant volume, the

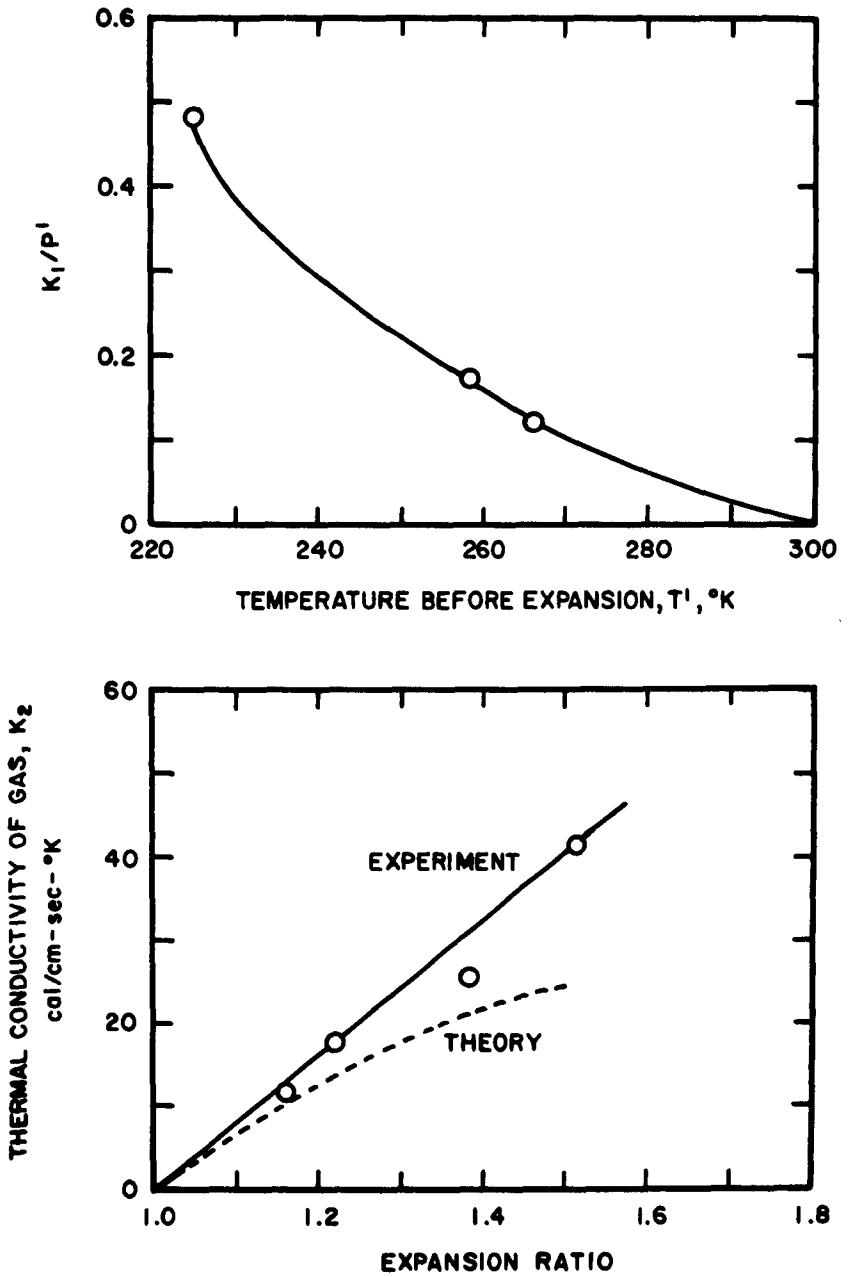

FIGURE 26. SUMMARY OF HEAT CONDUCTION IN CLOUD CHAMBER

previous report (1) noted that

$$\left.\begin{aligned} T_t &= T_o + \frac{\Delta H_s\, n_s}{\beta_z n_z + \beta_v n + \beta_s n_s} \\ &= T_o + \Delta H_s \left[\frac{n_o - n}{\beta_z n_z + \beta_s n_o - (\beta_s - \beta_v) n} \right] \end{aligned}\right\} \qquad (5)$$

where T_t and T_o are the temperatures at t = t and t = 0, ΔH_s is the heat of condensation of vapor to form solid, β_i is the constant-volume heat capacity of the i-th species, n_i is the number of moles of the i-th species, and n and n_o are the number of moles of the condensable vapor at t = t and t = 0. A liquid condensed phase merely requires replacing the subscript s by 1.

At a first approximation the temperature increase in the bulk phase due to heat conduction (Equation 1) may be taken as an <u>additive</u> correction to Equation 5. This is only an approximation since Equation 1 presumes isentropic heat conduction so that the adiabatic PVT laws can be used and since the available volume in the chamber actually is decreasing because of the heat conduction from the hot walls. However, this approximation gives the pressure at time t as (condensed phase = liquid):

$$P_t = \frac{(760)\,(0.08205)}{V}\,(n_z + n) \cdot$$

$$\left[T_0 + \Delta H_1 \left(\frac{n_0 - n}{\beta_z n_z + \beta_1 n_0 - (\beta_1 - \beta_v) n} \right) + K_2 t^{1/2} \right] \qquad (6)$$

The technique for analyzing the experimental pressure-time curve for condensation is as follows:

1. For a particular condensation run, the volume of the expanded chamber, K_2, and other parameters are incorporated into Equation 6.

2. A voltage and time are measured for a point on the Polaroid photograph or a magnified version.

3. The abolute pressure corresponding to this voltage is calculated by Equation 135 in reference 1.

4. The moles of gas, n, are calculated by Equation 6 by successive approximation (Equation 6 converts to a quadratic in n, but this approach is cumbersome).

5. The partial pressure of H_2O vapor at this time t is calculated from n, V, and the corresponding T (the bracketed term in Equation 6) by the ideal gas law.

6. The vapor pressure of bulk liquid water, p_e, at this T is calculated by Equation 120 in reference 1.

7. Finally, the supersaturation at this time t is given by

$$S = p/p_e$$

This procedure is done for a succession of voltage points measured from the experimental curve. An experimental supersaturation-time curve is constructed and may be compared to the theoretical S-t curve computed for the initial S and T in the cloud chamber.

2. Exact Approach. Since condensation is nonisentropic, the vapor temperature during piston bounce and heat conduction is not truly given by an adiabatic type of calculation. This true vapor temperature can be calculated as below.

The energy equation for a reacting gas mixture containing i species is (5)

$$dH = VdP = \Sigma\, (\Delta H_f)_i dn_i + \Sigma\, n_i \beta_i dT$$

where H is the enthalpy of the mixture, $(\Delta H_f)_i$ is the heat of formation, n_i is the number of moles of the i-th species, β_i' is the heat capacity at constant pressure of the i-th species, and T is the temperature. For the present water vapor-liquid water-argon mixture, the energy equation is

$$VdP = (\Delta H_f)_l\, dn_l + (\Delta H_f)_v\, dn + (\Delta H_f)_z\, dn_z + (\beta_z' n_z + \beta_l' n_l + \beta' n)\, dT \qquad (7)$$

Since $n_l = n_0 - n$ and $dn_z = 0$, Equation 7 becomes

$$VdP = [(\Delta H_f)_v - (\Delta H_f)_l]\, dn + [\beta_z' n_z + \beta_l' n_0 + (\beta' - \beta_l')\, n]\, dT \qquad (8a)$$

$$VdP = -\Delta H_1\, dn + [\beta'_z n_z + \beta'_1 n_0 - (\beta'_1 - \beta)n]dT \tag{8b}$$

Dividing by the coefficient of the dT term, integrating from t = 0 to t = t, and rearranging gives

$$\left.\begin{aligned} T_t &= T_0 + \Delta H_1 \int_{n = n_0}^{n = n_t} \frac{dn}{\beta'_z n_z + \beta'_1 n_0 - (\beta'_1 - \beta')n} \\ &\quad + \int_{P = P_0}^{P = P_t} \frac{VdP}{\beta'_z + \beta'_1 n_0 - (\beta'_1 - \beta)n} \\ T_t &= T_0 + \frac{\Delta H_1}{(\beta' - \beta'_1)} \ln\left(\frac{\beta'_z n_z + \beta'_1 n_0 - (\beta'_1 - \beta')n}{\beta'_z n_z + \beta' n_0}\right) \\ &\quad + \int_{P = P_0}^{P = P_t} \frac{VdP}{\beta'_z n_z + \beta'_1 n_0 - (\beta'_1 - \beta')n} \end{aligned}\right\} \tag{9}$$

The above equation is to be compared with Equation 5.

Now, for a given expansion ratio and also for a given cloud chamber, V is a function of t due to piston bounce and heat conduction. Since the volume change due to heat conduction is negligible during the time involved in piston bounce, these two effects may be separated, or

$$\begin{aligned} V = V(t) &= \text{volume at time } t \\ &= q(\text{piston bounce}) + r(\text{heat conduction}) \end{aligned}$$

These functions q and r can be calculated from experimental curves of P versus t obtained during expansion of <u>dry</u> argon. The function q typically would be the P_t versus t equation noted at the beginning of this section. The function r would be the $t^{1/2}$ equation in Equation 2.

Therefore, Equation 9 becomes

$$T_t = T_0 + \frac{\Delta H_1}{\beta' - \beta'_1} \ln\left(\frac{\beta'_z n_z + \beta'_1 n_0 + (\beta' - \beta'_1)n}{\beta'_z n_z + \beta' n_0}\right)$$

$$+ \int_{t=0}^{t=t} \frac{(q + r)\,dP}{\beta_z' n_z + \beta_1' n_0 + (\beta' - \beta_1')\,n} \tag{10}$$

and finally,

$$P_t = \frac{R}{V}(n_z + n)\left[T_0 + \frac{\Delta H_1}{\beta' - \beta_1'} \ln\left(\frac{\beta_z' n_z + \beta_1' n_0 + (\beta' - \beta_1')\,n}{\beta_z' n_z + \beta' n_0}\right) + \int_0^t \frac{(q + r)\,dP_t}{\beta_z' n_z + \beta_1' n_0 + (\beta' - \beta_1')\,n}\right] \tag{11}$$

Equation 11 may be compared with Equation 6 for the approximate case.

All parameters in Equation 11 are known except the values for n which satisfy the experimental values of P_t. If the integral in Equation 11 is converted to intervals, Equation 11 may be solved for n during each successive time interval by successive approximations. Each value of n is then converted to S by the technique noted previously.

Typical Calculation

No exact calculations have been made as yet. Results of the approximate calculation of the supersaturation-time curve for the condensation run presented as Figure 47 in reference 1 are given here. The conditions immediately after expansion are (corrected from Figure 47):

$$S_1 = 7.70$$

Chamber temperature = 259.5°K (after expansion)

Chamber pressure = 553.7 mm (after expansion)

The pressure immediately before and during piston bounce during the dry expansion and the corresponding supersaturation and temperature were given in Figure 18 assuming no condensation. The value of k_2 for an expansion ratio of 1.220 was taken from Figure 23.

The resulting supersaturation-time and temperature-time curves after the piston bounce were then calculated as noted earlier and are given in Figure 27.

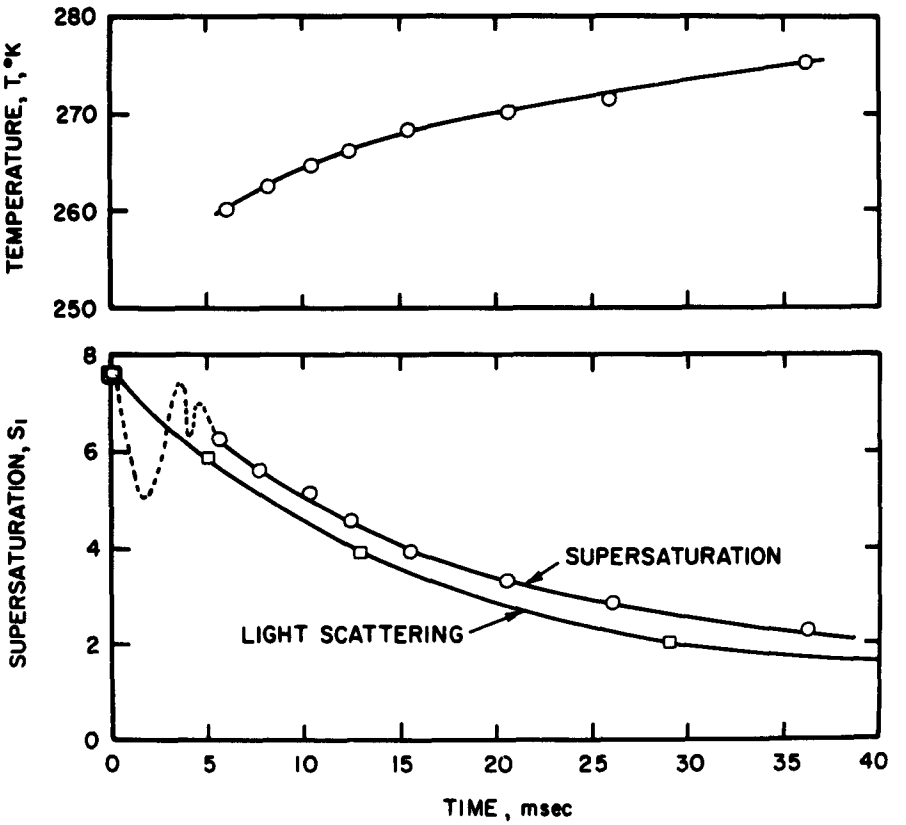

FIGURE 27. EXPERIMENTAL SUPERSATURATION-TIME AND TEMPERATURE-TIME CURVES

APPROXIMATE

For comparison, the upper envelope to the scattering-time curve was measured, normalized to the supersaturation at zero time and infinity, and superimposed on the above plot. The agreement between the supersaturation and scattering curves is better than might be expected.

Theoretical curves are currently being calculated by the author.

ACKNOWLEDGMENTS

The generalized steady-state nucleation problem was programmed by Mrs. Margaret Sullivan and run on the General Precision Computer RPC 4000 at TEI.

The experimental work was done by Kent Renalds.

REFERENCES

(1) W. G. Courtney, "Kinetics of Condensation from the Vapor Phase," Texaco Experiment Incorporated TM-1340, 15 July 1962.

(2) W. G. Courtney and W. J. Clark, "Kinetics of Condensation from the Vapor Phase," Texaco Experiment Incorporated TM-1250, 15 July 1961.

(3) W. G. Courtney, J. Chem. Phys., 35, 2249 (1961).

(4) W. E. Hazen, Rev. Sci. Instr., 13, 247 (1942).

(5) B. Lewis, R. N. Pease, and H. S. Taylor, Combustion Processes, p. 33, Princeton, Princeton University Press, 1956.

APPENDIX

Some representative samples of the experimental pressure-time curves obtained during condensation in the cloud chamber are given in Figures 28 through 38.

	BEFORE EXPANSION			EXPANSION RATIO	AFTER EXPANSION	
	T*, °C	T', °C	P', mm		T_o, °K	S_i
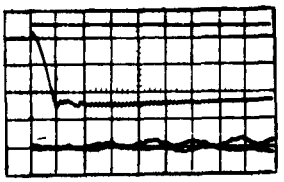	19.3	20.3	760.8	1.211	259.6	7.6
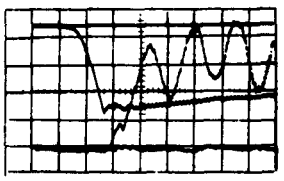	19.3	20.3	760.8	1.224	257.2	9.1
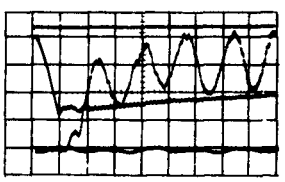	19.3	20.3	760.8	1.224	257.2	9.1
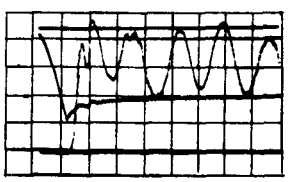	19.3	20.3	760.8	1.237	255.7	9.9

FIGURE 28. CONDENSATION OF WATER FROM ARGON SATURATED AT 20°C

T* SATURATOR TEMPERATURE
T' CHAMBER TEMPERATURE
T_o INITIAL TEMPERATURE AFTER EXPANSION
P' CHAMBER PRESSURE

SCALE: HORIZONTAL — 1 unit = 5 msec
VERTICAL — PRESSURE, 1 unit = 1 volt (SEE TEXT)
SCATTERING, 1 unit = 5 volts (ARBITRARY)

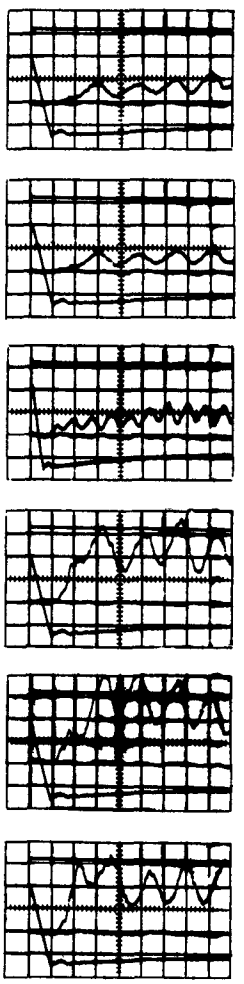

BEFORE EXPANSION			EXPANSION RATIO	AFTER EXPANSION	
T^*, °C	T^1, °C	P^1, mm		T_0, °K	S_1
0	20.0	760.2	1.382	237.1	12.7
0	20.2	760.2	1.382	237.2	12.5
0	20.5	760.2	1.382	237.5	12.2
(HORIZONTAL SCALE: 1 UNIT = 10 msec)					
0	20.8	760.2	1.395	235.6	14.6
0	20.5	760.2	1.395	235.6	14.6
0	20.5	760.2	1.395	235.6	14.6

FIGURE 29. CONDENSATION OF WATER FROM ARGON SATURATED AT 0°C

T^* SATURATOR TEMPERATURE
T^1 CHAMBER TEMPERATURE
T_0 INITIAL TEMPERATURE AFTER EXPANSION
P^1 CHAMBER PRESSURE

SCALE: HORIZONTAL — 1 unit = 5 msec
VERTICAL — PRESSURE, 1 unit = 1 volt (SEE TEXT)
SCATTERING, 1 unit = 5 volts (ARBITRARY)

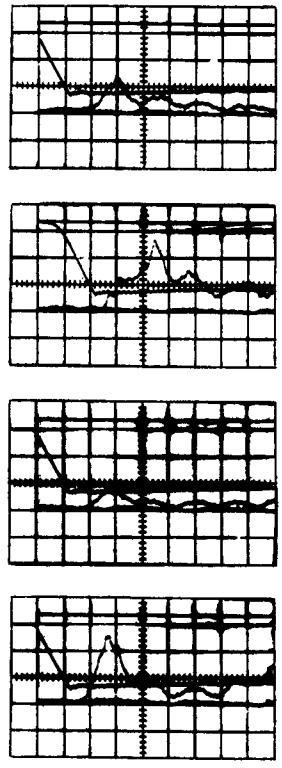

BEFORE EXPANSION			EXPANSION RATIO	AFTER EXPANSION	
T*, °C	T', °C	P', mm		T_o, °K	S_i
-8.0	23.0	759.1	1.500	226.7	18.0
-8.2	23.1	759.1	1.500	226.7	17.7
-10.0	23.0	759.1	1.513	225.4	17.5
-10.2	23.0	759.1	1.526	225.4	17.3

FIGURE 30. CONDENSATION OF WATER FROM ARGON SATURATED AT -10°C

T* SATURATOR TEMPERATURE
T' CHAMBER TEMPERATURE
T_o INITIAL TEMPERATURE AFTER EXPANSION
P' CHAMBER PRESSURE

SCALE: HORIZONTAL —— 1 unit = 5 msec
VERTICAL —— PRESSURE, 1 unit = 2 volts (SEE TEXT)
SCATTERING, 1 unit = 5 volts (ARBITRARY)

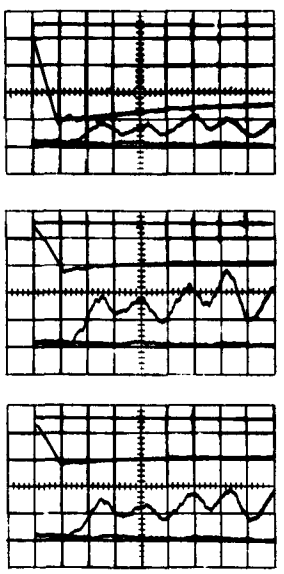

	BEFORE EXPANSION			EXPANSION RATIO	AFTER EXPANSION	
	T^*, °C	T^1, °C	P^1, mm		T_o, °K	S_i
A.	18.1	22.5	382	1.278	252.1	6.18
B.	18.1	22.5	382	1.291	250.5	6.92
C.	18.1	22.5	382	1.291	250.5	6.92

FIGURE 31. EFFECT OF ARGON PRESSURE ON CONDENSATION OF WATER

T^* SATURATOR TEMPERATURE
T^1 CHAMBER TEMPERATURE
T_o INITIAL TEMPERATURE AFTER EXPANSION
P^1 CHAMBER PRESSURE

SCALE: HORIZONTAL — 1 unit = 5 msec
VERTICAL — PRESSURE, 1 unit = 0.5 volt (A), 1.0 volt (B,C)
SCATTERING, 1 unit = 5 volts (ARBITRARY)

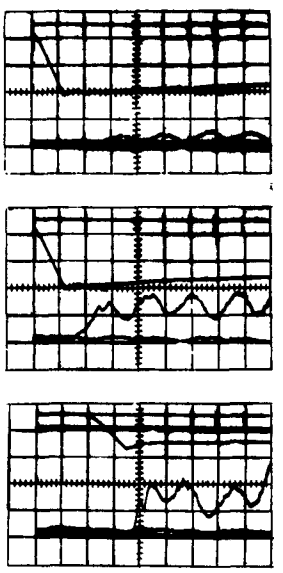

	BEFORE EXPANSION			EXPANSION	AFTER EXPANSION	
	T^*, °C	T^1, °C	P^1, mm	RATIO	T_o, °K	S_1
A.	24.0	18.0	225	1.357	243.9	7.01
B.	24.0	18.0	225	1.357	243.9	7.01
C.	24.0	18.0	225	1.357	243.9	7.01

FIGURE 32. EFFECT OF ARGON PRESSURE ON CONDENSATION OF WATER

T^* SATURATOR TEMPERATURE
T^1 CHAMBER TEMPERATURE
T_o INITIAL TEMPERATURE AFTER EXPANSION
P^1 CHAMBER PRESSURE

SCALE: HORIZONTAL — 1 unit = 5 msec
VERTICAL — PRESSURE, 1 unit = 0.5 volt (A,B), 1.0 volt (C)
SCATTERING, 1 unit = 5 volts (ARBITRARY)

	BEFORE EXPANSION			EXPANSION	AFTER EXPANSION	
	T^*, °C	T^1, °C	P^1, mm	RATIO	T_0, °K	S_1
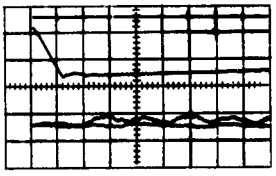	22.2	25.3	767	1.434	258.3	8.35
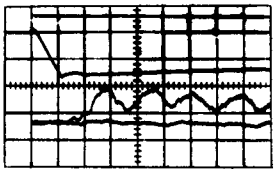	22.0	24.7	767	1.448	256.5	9.26
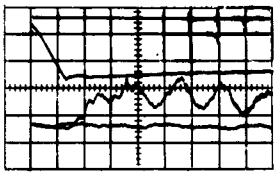	22.0	24.7	767	1.448	256.5	9.26

FIGURE 33. CONDENSATION OF WATER FROM NITROGEN SATURATED AT 20°C

T^* SATURATOR TEMPERATURE
T^1 CHAMBER TEMPERATURE
T_0 INITIAL TEMPERATURE AFTER EXPANSION
P^1 CHAMBER PRESSURE

SCALE: HORIZONTAL — 1 unit = 5 msec
VERTICAL — PRESSURE, 1 unit = 1 volt (SEE TEXT)
SCATTERING, 1 unit = 5 volts (ARBITRARY)

	BEFORE EXPANSION			EXPANSION RATIO	AFTER EXPANSION	
	T*, °C	T', °C	P', mm		T_o, °K	S_i
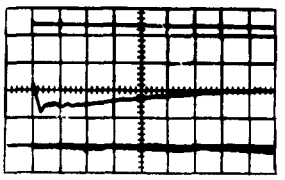	18.0	21.3	765.4	1.239	255.9	9.2
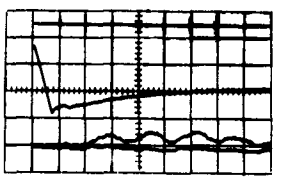	18.0	23.5	763.5	1.257	255.4	9.60
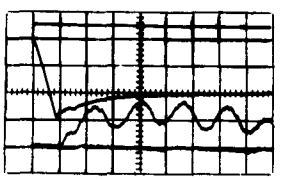	18.0	23.5	763.5	1.265	254.3	10.1
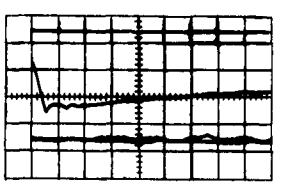	18.0	18.0	765.4	1.226	254.8	10.3
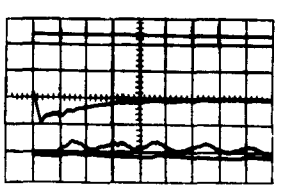	18.0	21.3	765.4	1.252	254.1	10.5

FIGURE 34. CONDENSATION OF WATER FROM HELIUM SATURATED AT 20°C

T* SATURATOR TEMPERATURE
T' CHAMBER TEMPERATURE
T_o INITIAL TEMPERATURE AFTER EXPANSION
P' CHAMBER PRESSURE

SCALE: HORIZONTAL — 1 unit = 5 msec
VERTICAL — PRESSURE, 1 unit = 1 volt (SEE TEXT)
SCATTERING, 1 unit = 5 volts (ARBITRARY)

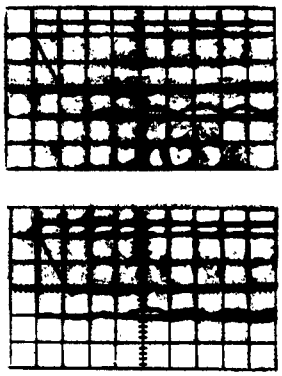

BEFORE EXPANSION			EXPANSION RATIO	AFTER EXPANSION	
T^*, °C	T^I, °C	P^I, mm		T_0, °K	S_I
-10.0	19.0	768.5	1.526	220.1	30.9
-10.0	19.0	768.5	1.526	220.1	30.9

FIGURE 35. CONDENSATION OF WATER FROM HELIUM SATURATED AT -10°C

T^* SATURATOR TEMPERATURE
T^I CHAMBER TEMPERATURE
T_0 INITIAL TEMPERATURE AFTER EXPANSION
P^I CHAMBER PRESSURE

SCALE: HORIZONTAL — 1 unit = 5 msec
VERTICAL — PRESSURE, 1 unit = 2 volts (SEE TEXT)
SCATTERING, 1 unit = 5 volts (ARBITRARY)

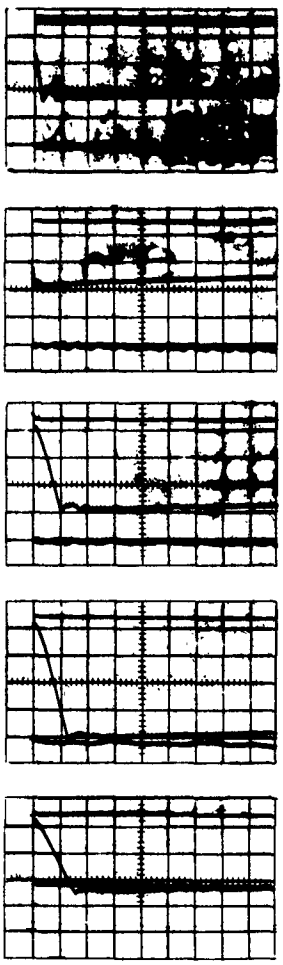

BEFORE EXPANSION T', °C	BEFORE EXPANSION P', mm	EXPANSION RATIO
19.3	760.8	1.092
19.3	760.8	1.158
(TIME: 1 UNIT = 20 msec)		
19.3	760.8	1.237
19.3	760.8	1.356
19.3	760.8	1.553
(PRESSURE: 1 UNIT = 2 volts)		

FIGURE 36. EXPANSION OF DRY ARGON INITIALLY AT 1 ATM

T' CHAMBER TEMPERATURE P' CHAMBER PRESSURE

SCALE: HORIZONTAL — 1 unit = 5 msec
VERTICAL — PRESSURE, 1 unit = 1 volt (SEE TEXT)
SCATTERING, 1 unit = 5 volts (ARBITRARY)

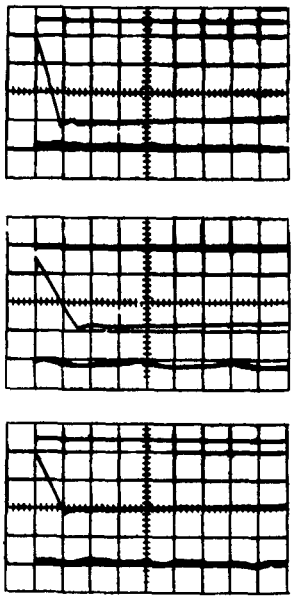

	BEFORE EXPANSION		EXPANSION RATIO
	T^1, °C	P^1, mm	
A.	22.1	382	1.278
B.	23.0	386	1.491
C.	25.1	18.3	1.357

FIGURE 37. EXPANSION OF DRY ARGON INITIALLY AT 1/2 AND 1/3 ATM

T^1 CHAMBER TEMPERATURE P^1 CHAMBER PRESSURE

SCALE: HORIZONTAL — 1 unit = 5 msec
VERTICAL — PRESSURE, 1 unit = 0.5 volt (A,C), 1 volt (B)
SCATTERING, 1 unit = 5 volts (ARBITRARY)

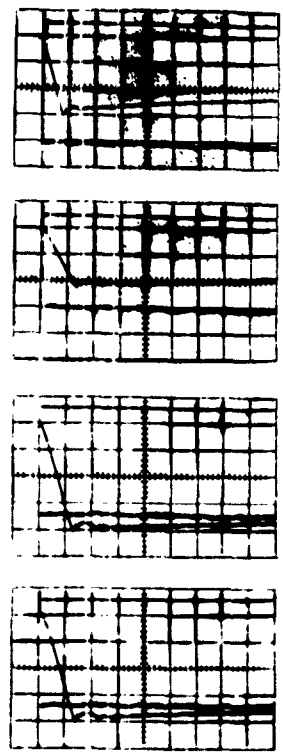

GAS	BEFORE EXPANSION T', °C	BEFORE EXPANSION P', mm	EXPANSION RATIO
He	23.1	763.5	1.235
He	19.0	768.5	1.526
(PRESSURE: 1 UNIT = 2 volts)			
N_2	22.7	767	1.448
N_2	22.7	767	1.434

FIGURE 38. EXPANSION OF DRY HELIUM AND NITROGEN INITIALLY AT 1 ATM

T' CHAMBER TEMPERATURE P' CHAMBER PRESSURE

SCALE: HORIZONTAL — 1 unit = 5 msec
VERTICAL — PRESSURE, 1 unit = 1 volt (SEE TEXT)
SCATTERING, 1 unit = 5 volts (ARBITRARY)